

Université de Montréal

**Characterization of in vivo vertebral growth modulation  
by shape memory alloy staples on a porcine model for the  
correction of the scoliosis**

par

Yaroslav Wakula

Département de sciences biomédicales

*Faculté de Médecine*

Mémoire présenté à la Faculté de Médecine

en vue de l'obtention du grade de M.Sc.

en Sciences Biomédicales

option Musculo-squelettique

Septembre 2012

© Yaroslav Wakula, 2012

Université de Montréal  
Faculté des études supérieures et postdoctorales

Ce mémoire intitulé :

**Characterization of in vivo vertebral growth modulation  
by shape memory alloy staples on a porcine model for the  
correction of the scoliosis**

Présenté par :  
Yaroslav Wakula

a été évalué par un jury composé des personnes suivantes :

Maxime Raison, président-rapporteur

Stefan Parent, directeur de recherche

Isabelle Villemure, co-directeur

Patrick Lavigne, membre du jury

## Résumé

La recherche de nouvelles voies de correction de la scoliose idiopathique a une longue histoire. Le traitement conventionnel de la scoliose idiopathique est présenté par le port du corset ou par la correction opératoire de la déformation. Depuis leur introduction, les deux méthodes ont prouvé leur efficacité. Cependant, malgré des caractéristiques positives évidentes, ces méthodes peuvent causer un nombre important d'effets indésirables sur la santé du patient. Les techniques sans fusion pour le traitement de la scoliose semblent être une alternative perspective de traitement traditionnel, car ils apportent moins de risques et des complications chirurgicales que les méthodes conventionnelles avec la conservation de la mobilité du disque intravertébral. Cependant, l'utilisation de techniques mentionnées exige une connaissance profonde de la modulation de croissance vertébrale. L'objectif principal de la présente étude est d'estimer le potentiel d'agrafes à l'AMF de moduler la croissance des vertèbres porcines en mesurant la croissance osseuse sur la plaque de croissance de vertèbres instrumentées en comparaison avec le groupe contrôle. La méthode est basée sur la loi de Hueter-Volkman. Nous avons choisi NiTi agrafes à l'AMF pour notre étude et les porcs de race Landrace comme un animal expérimental. Les agrafes ont été insérés sur 5 niveaux thoracique de T6 à T11. En outre, les radiographies ont été prises toutes les 2 semaines. La présence d'agrafes en alliage à mémoire de forme a produit la création de courbes scoliotiques significatives dans 4 de 6 animaux chargés et le ralentissement considérable de la croissance osseuse (jusqu'à 35,4%) comparativement aux groupes contrôle et sham. L'étude a démontré in vivo le potentiel d'agrafes en alliage à mémoire de formes de moduler la croissance des vertèbres en créant des courbes scoliotiques sur les radiographies et en ralentissant le taux de croissance sur les plaques de croissance instrumenté. La position précise de l'agrafe est essentielle pour la modulation de croissance osseuse et le développement de la scoliose expérimentale.

**Mots-clés:** agrafes en alliage à mémoire de formes, la modulation de croissance, le traitement sans fusion, scoliose.

## ABSTRACT

The search for a new ways of correction of idiopathic scoliosis was started long ago. Conventional treatments of idiopathic scoliosis comprise predominantly bracing and open correction of the deformity. Since their introduction, both methods have proven effective. However, despite evident positive characteristics, these methods can pose a significant number of undesirable effects to patient health.. There for fusionless techniques for the treatment of scoliosis seems to be a perspective alternative of traditional treatment as it presents less surgical risks and complications then conventional methods including maintenance of disc mobility. However the use of mentioned techniques demands a deep knowledge of vertebral growth modulation. The principal objective of present study is to estimate the potential of SMA staples to modulate the growth of porcine vertebrae by measuring bone growth on the growth plate of instrumented vertebrae in comparison with the control group.

The method is based on the Hueter-Volkman law. We choose NiTi SMA staples for our study and Landrace domestic pigs as an experimental animal. The staples were inserted on 5 thoracic levels from T6 to T11. Additionally, radiographs were taken every 2 weeks.

The presence of shape memory alloy staples led to creation of significant scoliosis curves in 4 of 6 loaded animals and considerable slowing of bone growth (up to 35.4.%) comparatively to control and sham groups.

The study has demonstrated in vivo the potential of the shape memory alloy staples to modulate the growth of vertebrae by creating scoliotic curves on radiographs and by slowing the growth rate on the instrumented growth plates. Accurate position of the staple is essential for the bone growth modulation and the development of experimental scoliosis.

**Keywords** : Shape memory alloy staples, growth modulation, fusionless treatment, scoliosis.

## CONTENTS

Title .....	i
Members of jury .....	ii
Résumé .....	iii
Abstract .....	iv
Contents .....	v
List of abbreviations.....	viii
List of tables .....	ix
Liste of figures .....	x
Dedication .....	xii
Acknowledgement .....	xiii
Introduction .....	xiv
CHAPTER 1 Literature overview .....	1
1.1 Bone growth .....	1
1.1.1 Morphology of the Growth Plate .....	1
1.2 Scoliosis .....	2
1.2.1 Prevalence .....	3
1.2.2 Etiology .....	3
1.2.3 Natural history.....	4
1.2.4 Classification .....	5
1.2.4.1 Cobb angle.....	5
1.2.4.2 King-Moe classification.....	6
1.2.4.3 Lenke classification.....	7
1.2.5 Management .....	8
1.2.5.1 Bracing.....	9
1.2.5.2 Surgical treatment.....	9
1.3 Experimental methods of growth modulation .....	11
1.3.1 T.Braun, M.D. et al.....	11
1.3.2 Peter O. Newton M.D. et al.....	12

1.3.3	Donita Bylski-Austrow, Eric Wall et al.....	14
1.3.4	Randal R. Betz MD et al.....	16
1.3.5	Ian A.F. Stokes et al.....	18
1.4	General conclusion.....	19
CHARTER 2 Objectives and Hypotheses.....		20
CHARTER 3 Materials and Methods .....		21
3.1	Introduction .....	21
3.2	Animal model.....	21
3.3	Surgical protocol .....	23
3.4	Radiographic control.....	25
3.5	Growth plate labelling.....	26
3.5.1	Plasticisation of vertebrae and cutting .....	26
3.5.2	Growth rate measurement .....	28
3.6	Statistical analyses .....	29
CHAPTER 4 Scientific article .....		30
4.1	Characterization of in vivo vertebral growth modulation by shape memory alloy staples on a porcine model for the correction of the scoliosis .....	30
4.1.1	Structured Abstract.....	32
4.1.2	Introduction .....	33
4.1.3	Materials and Methods.....	34
4.1.3.1	Surgical Protocol.....	35
4.1.3.2	Radiographic control.....	36
4.1.3.3	Bone growth labelling and tissue preparation.....	36
4.1.3.4	Growth rate measurement.....	37
4.1.3.5	Statistical analyses.....	38
4.1.4	Results .....	39
4.1.4.1	Radiographs.....	39
4.1.4.2	Bone growth measurement.....	40

4.1.5	Discussion .....	40
4.1.6	References: .....	42
CHAPTER 5	Results .....	44
5.1	General information .....	44
5.2	Radiographic control .....	44
5.3	Bone growth measurement.....	46
CHAPTER 6	Discussion .....	<b>Fehler! Textmarke nicht definiert.</b>
CHAPTER 7	Conclusion .....	53
References	.....	55
Annexe 1	.....	59
1.1	The descriptive anatomy of spine. ....	59
1.1.1	Cervical spine.....	60
1.1.2	Thoracic spine .....	61
1.1.3	Lumbar spine.....	62
1.1.4	Sacrum.....	62
1.1.5	Coccyx.....	63
1.1.6	Structure and function of intervertebral discs .....	64
1.1.7	Ligaments of the spine .....	65

**LIST OF ABBREVIATIONS**

AIS	adolescent idiopathic scoliosis
CT	computed tomography
GP	growth plate
I/M	intramuscular
IS	idiopathic scoliosis
I/V	intravenous
IV	intervertebral (disc)
LAT	lateral projection
MPa	megapascal
NiTi	nickel-titanium alloy (nitinol)
PA	posterior-anterior projection
SC	spinal column
SMA	shape memory alloy
UV	ultraviolet



**LIST OF TABLES**

<i>Table 3.1. Plasticisation of vertebrae</i> .....	27
<i>Table 4.1. Cobb angle in all groups.</i> .....	39
<i>Table 5.1. Cobb angles in three groups of animals.</i> .....	45
<i>Table 5.2. Average growth rate in three groups of animals.</i> .....	46
<i>Table 5.3. Average growth rate in three groups of animals(zones 3and 4).....</i>	48
<i>Table A.1. The range of motion in cervical spine (males).</i> .....	60

## LIST OF FIGURES

Figure 1 1. Growth plate zones. ....	2
Figure 1.2. The ratio boys/girls by age.. ....	3
Figure 1.3. Risser's sign proceeds from grade 0 (no ossification) to grade 4 .....	5
Figure 1.4. Cobb method of measuring the degree of scoliosis. ....	6
Figure 1.5. King classification of scoliotic curves. ....	7
Figure 1.6(a, b). Brace types (a) Milwaukee, (b) Boston.....	9
Figure 1.7(a, b). Cotrel-Dubousset (a) and Luque (b) rod systems.....	10
Figure 1.8. Vertebral body stapling. ....	17
Figure 3.1. Experimental animal.....	21
Figure 3.2. Memory alloy staple. ....	22
Figure 3.3 (a, b). Posterior-anterior (a) and lateral (b) radiographs of porcine spine. ....	25
Figure 3.4 (a, b). Vertebra-disc-vertebra bloc (a) and sections (b). ....	27
Figure 3.5. Sequences A and B. ....	28
Figure 3.6. 4 zones of growth plates .....	28
Figure 3.7. Two fluorescent lines of calcein.....	29
Figure 4.1. Insertion of the staples.....	35
Figure 4.2. Two sequences of sections.. ....	37
Figure 4.3. Four zones of growth plate. ....	37
Figure 4.4. Growth plate under the microscope.....	38
Figure 4.5. Distribution of the growth rate in 4 zones. ....	41
Figure 5.1(a,b,c). The initial PA radiographs of thoracic spine of animals from a) control, b) loaded and c) sham groups.....	44
Figure 5.2. Diagrams representing an average growth rate in three groups of animals.....	46
Figure 5.3. Diagrams representing an average growth rate in three groups of animals (zones 3 and 4).....	47
Figure 5.4( a, b). Accurate positioning (a) of the staple has resulted in notable decrease (b) of growth rate in two neighbor growth plates.. ....	48

Figure 5.5(a, b). The staple is displaced (a). Only the distal T9 growth plate was compressed (b) .....	48
Figure 6.1. Final PA radiograph of thoracic spine of animal 6. The presence of 9° scoliosis curve.....	51
Figure 1.1 Schematic image of the spine. ....	59
Figure A.2 Cervical vertebrae.....	60
Figure A.3 Thoracic vertebrae. ....	61
Figure A.4 Lumbar vertebrae.....	62
Figure A.5 Sacrum and Coccyx.. ....	63
Figure A.6. Structure of intervertebral disc .....	64
Figure A.7. Ligaments of the spine.....	65

## **DEDICATION**

*To my mother, Alexandra.*

*Thank you for your presence and love. I will always keep you in my heart.*

## **Acknowledgment**

The realisation of this work would be impossible without a great support of my scientific director Stefan Parent and co-director Isabelle Villemure.

Dr. Stefan Parent was a key figure in this project. Without his experience in surgery and science it would be impossible to perform both experimental and theoretical parts of the study. Special thanks for his humanity and understanding of personal needs and problems of his students.

I am very grateful for all these years that I have spent in Laboratory of Paediatric Mechanobiology in Saint-Justine Hospital, where Dr. Villemure is a director. The friendly and inspiring atmosphere created by the director and the members of scientific team inside those walls has lead to the successful end of my work.

I would also to express my gratitude to other members of Saint-Justine Research Center, whose input to this work is more than just great. Special thanks to Mark Driscoll and his wife Jennifer Forbes for their enormous support with experiment and edition of my paper. Also, without help of Irene Londono, Josee Depot, Souad Rhalmi, Kim Sergerie, Samira Amini and Barthélémy Valteau it would be very difficult for me to end successfully the project.

## Introduction

Spinal deformities are known for the whole period of human history. Ancient works of philosophy, religion, myths, and fairy tales dating back as far as 3500 BC invoke images of people with spinal deformity [1]. The term scoliosis (from Ancient Greek: σκολιος skolios "crooked") was widely used even in times of Hippocrates (460-370 BC), he also was one of the first doctors who started to treat this condition [1]. With the development of medical science and the science in toto, the definition of scoliosis has evolved from simple "curve" to modern definition of scoliosis as a complex three dimensional spinal deformity that results from both known and unknown causes in patients of all ages [1]. Above all types of scoliosis, idiopathic scoliosis represents our point of interest as it's the most common type of spinal deformity, accounting for nearly 80% of patients with structural scoliosis [1].

Nowadays, conventional treatment of idiopathic scoliosis depends on the angle of the curve and its progression. However, whether a brace or an open reduction will be chosen for each particular patient, these methods often carry a number of undesirable side effects: the need of wearing a brace during many months or several years creates obvious difficulties for the patient that can affect his or her compliance; it lowers patient's self estimation and causes cosmetic problems. In case of operative treatment those effects are more serious: vast operative approach to the spine, significant traumatisation of tissues during the mobilisation and skeletisation of the spine, significant blood loss and need of transfusion, limited range of motion after the fusion and cosmetic defect. It is a great challenge for patient, his relatives as well for the treating doctor.

Because of the mentioned reasons, the search for new corrective methods of scoliotic curves is an important issue, in order to improve patient quality of life and to minimise the side effects of standard treatment. The search for a new, less invasive method of treatment had started almost in the same time as the rods were introduced into clinical practice. From our point of view, fusionless surgical treatment of scoliosis (such as SMA staples in our case) is a potentially effective alternative to the conventional surgical

procedures. It has a number of advantages such as: preservation of motions in the instrumented spine segment, less invasive procedure (in many cases can be held by endoscopic approach), less potential risks for the patient, possibility of growth after the surgery and more acceptable cosmetic defects.

However, such innovative approach to the patient needs a solid scientific background. Since the first works published in 1950s [1, 2] to the present time, a considerable number of data regarding fusionless methods of treatment was brought to light. All of them are based on a well-known principle called Hueter-Volkman Law [3, 4]. This law proposes that growth is retarded by increased mechanical compression, and accelerated by reduced loading in comparison with normal values [3, 4]. . The modulation of vertebral growth was achieved by application of different types of implants: rigid or flexible tethers (Peter O. Newton M.D and al., John T. Braun, MD and al.), custom made implants (Donita Bylski-Austrow, Eric Wall and al.), external Ilizarov fixator (Ian Stokes and al., M. Cancel and al.) and SMA staples. The last method wasn't just tried in animal studies, but also there is a group of researchers headed by Randal R. Betz MD and al. who used SMA staples to treat scoliosis in adolescents. We choose the same type of implants for our study because of its relative safety and simplicity in regard of instrumentation and because it was already used in humans.

This master degree project aims to demonstrate the potential of SMA staples to modulate the growth of porcine vertebrae on both microscopic and macroscopic scales. We measured the rate of vertebral growth on instrumented vertebral growth plate and estimated the development of scoliotic curve on the radiographs. We hope that by gathering these data we will approach more closely to the introducing of fusionless methods of treatment of scoliosis in clinical practice.

The present work consists of 5 chapters. The first chapter is a review of literature started with the descriptive anatomy of spine. The second part presents objectives and methods followed by scientific article, which is the third chapter. The last two chapters are results and discussion with conclusion.

## CHAPTER 1 Literature overview

*In this chapter we will review the bone growth, bone tissue morphology the methods of bone growth modulation. For the descriptive anatomy of spine and scoliosis please look: Annexe 1.*

### **1.1. Bone growth**

#### **1.1.1. Morphology of the Growth Plate**

The understanding of growth plate (GP) morphology and structure is important to a research study. The growth plate can be divided into a series of anatomic zones that represent unique morphological and biochemical stages during the process of chondrocyte differentiation. In the resting zone, the ratio of extracellular matrix to cell volume is high and the cells are in a relatively quiescent state. In the proliferating zone, chondrocytes assume a flattened appearance, begin to divide, and become organized into columns. In the zone of maturation, the synthesis of extracellular matrix allows the recently divided cells to separate from each other. This extracellular matrix consists predominantly of collagens and proteoglycans as well as other noncollagenous proteins [5, 6]. (Figure 1.1).



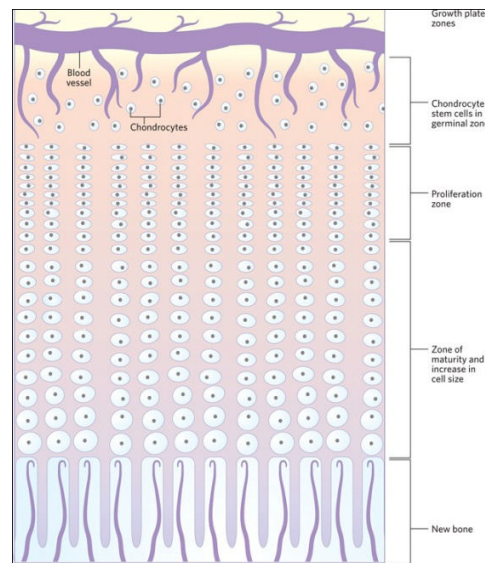


Figure 1. 1: Growth plate zones (adapted from [7]).

## 1.2. Scoliosis

In present time, the majority of authors define scoliosis as a complex three-dimensional deformity of the spine . Practically, three-dimensional refers to lateral bending of the spine combined with rotation of the affected vertebral segments. The most common type of scoliosis is idiopathic scoliosis accounting for nearly 80% of patients with structural scoliosis[5, 10]. The term idiopathic implies that a definitive cause of the disease has yet to be discovered. In younger patients, this type of spinal deformity can be divided into three groups based on age at onset of symptoms:

- 1) Infantile idiopathic scoliosis (0-3 years)
- 2) Juvenile idiopathic scoliosis (4-9 years)
- 3) Adolescent idiopathic scoliosis (10 years to the end of skeletal growth.)

Scoliosis revealed subsequent to the end of bone growth is defined as adult scoliosis.

Since adolescent idiopathic scoliosis (AIS) is the most common among those identified here, it deserves a more detailed overview[11].

### 1.2.1 Prevalence

Following numerous studies on the subject, researchers have come to the conclusion that sex of the patient plays an important role in the prevalence of AIS. The prevalence of radiographic curves measuring at least 10 degrees ranges from 1.5% to 3.0%, of curves exceeding 20 degrees from 0.3% and 0.5%, and of curves exceeding 30 degrees from 0.2% and 0.3%. The ratio of affected females to males (Figure 1.2) is 1:1 for curves between 6 and 10 degrees, 1.4:1 for curves between 11 and 20 degrees, 5.4:1 for curves exceeding 21 degrees but not requiring treatment, and 7.2:1 for curves requiring orthopaedic intervention [11, 12] .

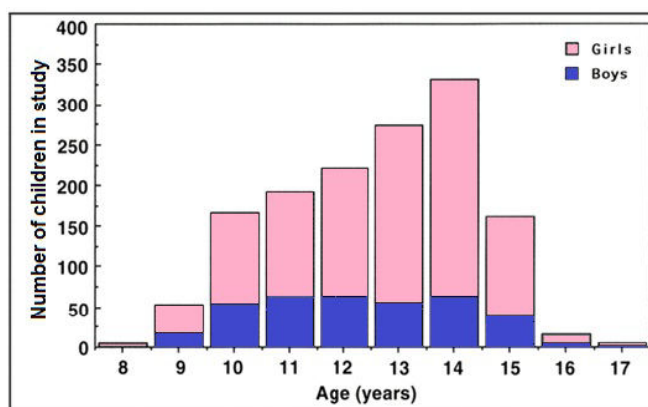


Figure 1.2: The ratio boys\girls by age (adapted from [9]).

### 1.2.2 Etiology

The definitive etiology of idiopathic scoliosis remains unknown. However, hereditary factors are proven to play a significant role in the development of this pathological condition. The studies conducted by Wynne-Devies in her family survey indicated that approximately one-fourth of patients with IS had a relative who was affected with scoliosis, although no clear mode of inheritance was discovered from the data [11].

### 1.2.3 Natural history

The majority of patients diagnosed with mild idiopathic scoliosis never experience problems as a result of their condition. Reports in the literature indicate that individuals with untreated curves less than 20 degrees are at low risk for progression, particularly as they approach skeletal maturity. Some patients, however, have curves that continue to progress over the years and ultimately lead to health problems. Thus, it is important to recognize the factors associated with curve progression; patient sex, remaining growth, curve magnitude, and curve pattern. Factors of no predictive value for curve progression before skeletal maturity include a family history of scoliosis, patient height-to-weight ratios, lumbosacral transitional anomalies, thoracic kyphosis, lumbar lordosis, and spinal balance [8]. In order to evaluate the possibility of progression of the curve, mainly two methods are used: Risser's sign (Figure 1.3) (a skeletal marker) and, in females, menarchal status (a physiologic marker). Risser's sign is a radiographic measurement based on the ossification of the iliac apophysis, which is divided into four quadrants. Risser's sign proceeds from grade 0, no ossification, to grade 4, in which all four quadrants of the apophysis show ossification ("capping"). Once the ossified apophysis has fused completely to the ilium (Risser grade 5), the patient is considered fully skeletally mature. Patients with Risser grade 0 or 1 (and, to a lesser extent, grade 2) are at the greatest risk for curve progression because a significant amount of spinal growth remains. Menarchal status is a clinical measurement applicable only to females. A premenarchal girl is still in the active growth period. Following menarche, she enters the deceleration phase of growth, and the likelihood of curve progression lessens [8].

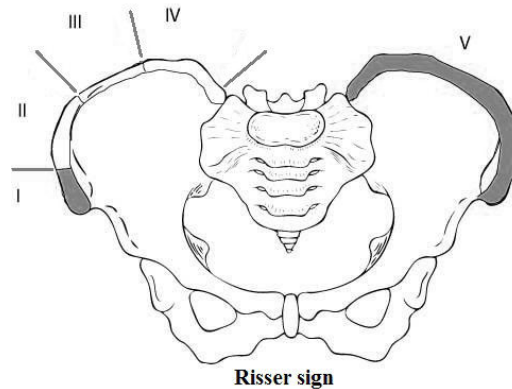


*Figure 1.3: Risser's sign proceeds from grade 0 (no ossification) to grade 4 (adapted from [13]).*

## **1.2.4 Classification**

### **1.2.4.1 Cobb angle**

There are several classification systems used in clinical practice. Radiography was, and remains, the basic diagnostic method in evaluating a scoliotic curve. Usually a standing posterior-anterior view of the patient's spine is necessary, additional views are taken as indicated. The Cobb method is used to measure the degree of scoliosis on the posterior-anterior radiograph (Figure 1.4). In addition to the degree, the curves should be described as "right" or "left," based on their curve convexity. Standard measurement error is 3 to 5 degrees for the same observer and 5 to 7 degrees for different observers when the same endvertebrae are used for measurements. Curves are named for the location of the apex vertebrae, and may be described as thoracic, lumbar, thoracolumbar, cervical, or double major (two curves in different spinal regions) [14, 15].

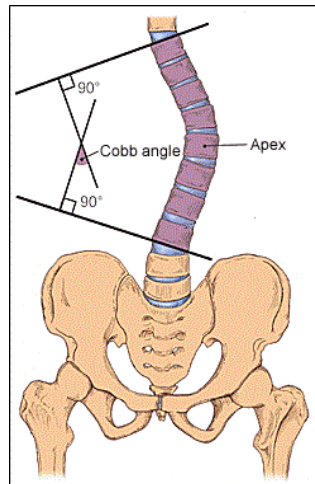


*Figure 1.4: Cobb method of measuring the degree of scoliosis (adapted from [15]).*

Curves less than 10 to 15 degrees are considered to be small, require no active treatment and are simply monitored, unless the patient's bones are very immature and progression is likely. Moderate curves, between 25 and 45 degrees, in patients lacking skeletal maturity have previously been treated with bracing. In patients with a curve severe enough to require surgery (greater than 45 degrees in adolescents and greater than 50 degrees in adults), rod placement and bone grafting may be necessary to achieve partial or complete correction [11, 15].

#### **1.2.4.2. King-Moe classification**

In 1983, King and colleagues introduced a radiographic classification system for adolescent idiopathic scoliosis in which five different curve types were described (Figure 1.5). The classification system determined the severity of a case based on Cobb angle and flexibility index from bending radiographs. King type I represents an S-shaped curve crossing the midline of the thoracic and lumbar curves. The lumbar curve is larger and more rigid than the thoracic curve. The flexibility index in the bending radiographs is negative. King type II is an S-shaped curve where both the thoracic major curve and the lumbar minor curve cross over the midline. The thoracic curve is larger. King type III represents a thoracic curve where the lumbar curve does not cross the midline. King type IV represents a long thoracic

curve where the fifth lumbar vertebra is centered over the sacrum, but the fourth lumbar vertebra is already angled in the direction of the curve. King type V represents a thoracic double curve where the first thoracic vertebra angles into the convexity of the upper curve. Together with its progressiveness this classification has its disadvantages:

- The sagittal profile is not included in the evaluation; and
- So-called “double and triple major curves” (scoliosis forms with two or three major curves) are not considered[5, 16].

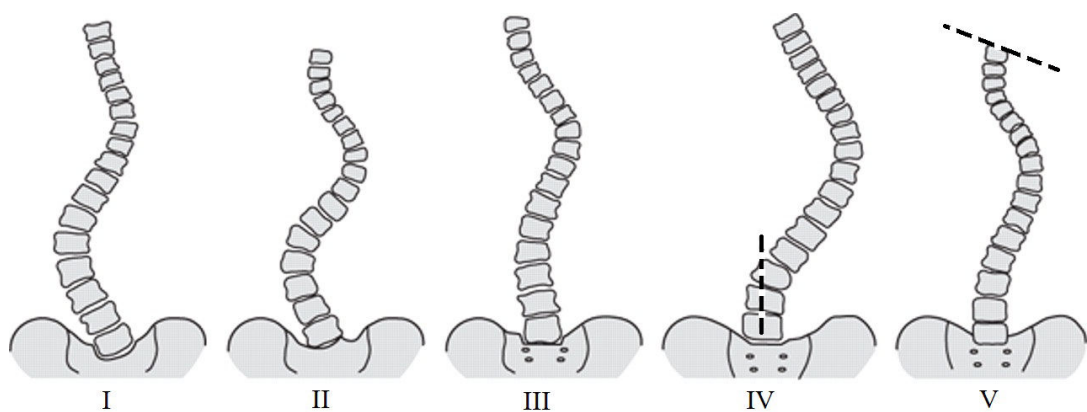


*Figure 1.5: King classification of scoliotic curves (adapted from [16]).*

### 1.2.4.3 Lenke classification

In 1997, Lenke introduced a new classification system, much more complex than the King system, for idiopathic scoliosis. Goals of the new classification system were, namely, to allow for more acceptable comparisons among the various types of operative treatments available, as to support a treatment-based approach to the patient. Determination of the scoliosis type is based on survey spine radiographs in two planes, as well as right and left side bending radiographs with the following parameters [5, 16].

The curve type is determined by the localization, degree, and flexibility of the manifested curves. For localization purposes, the curve apex is defined as:

- Upper thoracic localization: Curve apex between Th2 and Th6
- Thoracic localization: Curve apex between Th6 and intervertebral disc Th11/12

- Thoracolumbar localization: Curve apex between Th12 and L1
- Lumbar localization: Curve apex between intervertebral disc L1/2 and L4.

*Determination of the flexibility of the curve.*

The flexibility is assessed either based on the residual curve in the bending radiograph or the extent of kyphosis. A curve is defined as structural if the bending Cobb angle exceeds 25° or the kyphosis angle exceeds 20°.

The following six curve types can be defined using these parameters:

- Type I (main thoracic, major curve thoracic only)
  - The major curve is structural, the others are not.
- Type II (double thoracic, 2 thoracic curves)
  - The thoracic major curve and the upper thoracic minor curve are structural; all others are non- structural.
- Type III (double major, 2 major curves)
  - The thoracic, thoracolumbar or lumbar curve is structural; the thoracic curve is larger than the thoracolumbar or lumbar curve. If there is an upper thoracic curve, it is not structural.
- Type IV (triple major, 3 major curves)
  - All three curves are structural; the thoracic curve is the major curve.
- Type V (primary thoracolumbar/lumbar, major curve thoracolumbar or lumbar only)
  - The major curve is located in the thoracic-to-lumbar transition or in the lumbar spine and is structural; the upper thoracic or thoracic minor curve is not structural.
- Type VI (primary thoracolumbar/lumbar, main thoracic)
  - The thoracolumbar or lumbar major curve is structural; the thoracic minor curve is also structural, but its Cobb angle is at least 5° smaller[16].

### **1.2.5 Management**

Management of AIS is a complex process; the main goal is the prevention of the progression of scoliotic curves. The selection of a treatment method for each particular case depends predominantly on the severity of the curve. There are three therapeutic options:

- Observation
- Bracing
- Surgery

For curves between 0 and 20 degrees (Cobb angle), which represents the majority of patients with AIS, the sole option is observation.

### 1.2.5.1 Bracing

Based on the natural history of idiopathic curves, brace treatment should, in general, keep curves below 40 degrees or below the point at which they have the potential to cause an ill effect on the health of the patient[17]. The indications for bracing are: Cobb angle between 20 to 40 degrees, risk of progression, and cosmetic defect caused by the curve[18]. Corrected forces are provided during the external application of the brace, which concurrently correct the curve.. Below are two types of braces used in clinical practice (Figure 1.6).

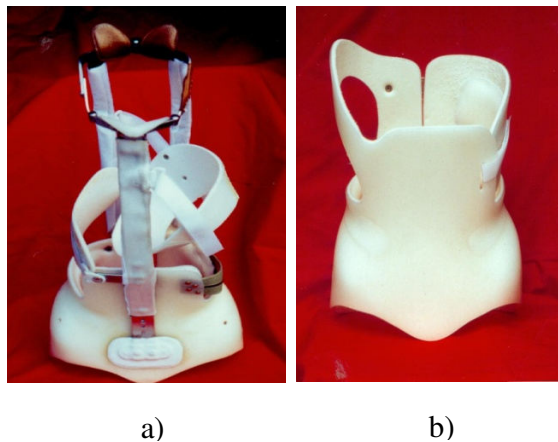


*Figure 1.6. Brace types (a) Milwaukee, (b) Boston (adapted from[19]).*

### 1.2.5.1 Surgical treatment

Indications of a need for surgical intervention in patients with AIS vary in each particular case, nonetheless there are certain basic criteria for such a clinical decision. The



strongest indication for surgery is a curve that reaches  $45^\circ$  to  $50^\circ$ . This is especially relevant to thoracic curves, due to evidence that progression continues subsequent to the completion of growth [20]. In the case of lumbar curves there are no respiratory problems, however once the curve exceeds  $60^\circ$  it can result in considerable back pain and should be treated [21]. Cosmetic defect is another non negligible reason for surgery, especially in female patients. Over the past several decades the choice of instrumentation system has changed from a simple Harrington rod to a variety of instruments used in present time. Most commonly, all past and present methods require fusion of affected vertebrae. The goals of instrumentation include the correction of the lateral curve, reduction of the rib hump, correction of rotation, rigidity of fixation to aid in obtaining fusion and safety. Recently, two criteria have become increasingly popular in the conventional treatment of AIS: the elimination of post operative immobilization and the correction of vertebral rotation. The first is responsible for the popularization of the Luque (Figure 1.7) method and the second for the Cotrel-Dubousset system [11]. Further to several studies undertaken by Dubousset [22] and Mullaji [23], it is better to postpone surgical intervention for as long as possible in an effort to further maturation of bone tissue

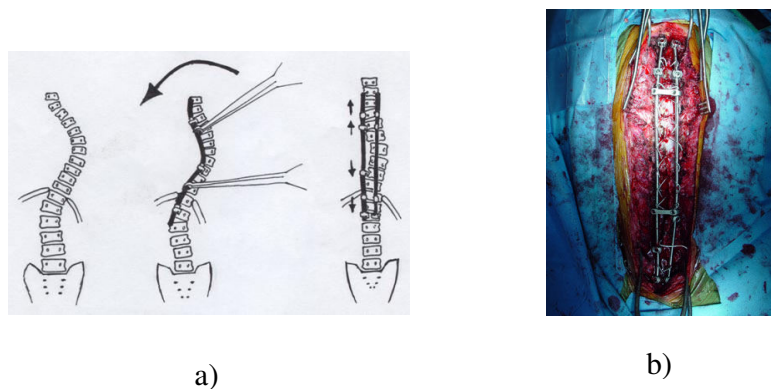


Figure 1.7. Cotrel-Dubousset (a) and Luque (b) rod systems (adapted from [24]).

### **1.3 Experimental methods of growth modulation**

Currently the operative treatment of choice for idiopathic scoliosis with a curve greater than 40° is, most often, open reduction through fusion of one or several spine segments using a rod system. However, this method often carries a number of undesirable side effects: vast operative approach to the spine, significant traumatisation of the tissues during the mobilisation and skeletisation of the spine, significant blood loss and need of transfusion, limited range of motion after the fusion, cosmetic defect, etc. Even a less invasive intervention, for example bracing, can create difficulties for the patient affecting his or her compliance. These are typically cosmetically based issues that may lead to feelings of decreased self-esteem. It is for these reasons that the pursuit of new methods for correcting scoliotic curves remains an important issue, both to improve patient quality of life and to minimize the side effects of standard treatment. Since the 1950s there have been attempts [2, 25] to find new methods to treat scoliosis using vertebral body stapling and other fusionless techniques. Fusionless surgical treatment of scoliosis is a potentially effective alternative to conventional surgical procedures. It has a number of advantages such as the preservation of motions in the instrumented spine segment, a less invasive procedure (in many cases it can be performed by endoscopic approach), fewer potential risks for the patient, the possibility of growth after the surgery, and more acceptable cosmetic defects. The following will provide an overview of recently published studies representing the main directions of different researchers on the subject of experimental methods for creating scoliotic curves.

#### **1.3.1 T.Braun, M.D. et al.**

Studies undertaken by a group of researchers and headed by John T. Braun, M.D. [26-29] led to the publication of a number of articles on the experimental methods of creating and correcting scoliosis using either anterior vertebral body stapling or anterior ligament tethers attached to bone anchors. The experimental animal model used in these studies was the Spanish X-crossed female goat, selected both for its overall size and size of

the components of its spine, similar to that of a juvenile human. At the beginning of the study the animals were 6-8 weeks in age and weighed between 6.4-11.8 kg. Two methods were used to create scoliosis deformity.

#### *Rigid posterior asymmetric tethering*

This method was used in 40 goats [29]. Of the animals that survived, 82 % developed progressive, structured idiopathic type curves convex to the right thoracic spine. Six of 33 animals failed to develop a scoliotic curve. Following the procedure, the average initial curves measured 42° and increased to 60° over the six to 15 week tethering period.

#### *Flexible posterior asymmetric tethering*

This method was used in 24 goats. Of the animals that survived, 91 % developed progressive structural, lordoscoliotic curves. The curves increased from an initial average of 55.4 ° to 74.4° over an eight week tethering period. Both groups of animals were later used for the correction of experimental scoliosis through two methods: anterior thoracic stapling and bone anchors with ligament tethers..

#### *Results*

In both groups the authors observed correction of scoliosis after the application of staples: 14° for the first group and from the average of 73.4° ± 8.4° to 69.9° ± 9.7° for the second. The conclusion was made that anterior vertebral body stapling is an effective method for the correction of moderately severe scoliosis deformity in a goat model. Greater correction was observed in the stapled goats versus untreated [28].

### **1.3.2 Peter O. Newton M.D. et al.**

A group of researchers from the University of California headed by Peter O. Newton M.D. performed several studies using flexible tether, either steel or polyethylene,

to create an experimental scoliosis in porcine and bovine models [30-31]. The first study was held using a porcine model for growth modulation [31].

#### *Description of study*

Twelve seven-month-old mini-pigs underwent instrumentation with a vertebral staple-screw construct connected by a polyethylene tether over four consecutive thoracic vertebrae. The instrumented levels were from T8 to T11. Monthly radiographs, computed tomography and magnetic resonance imaging scans (made after the spines were harvested), histological findings, and biomechanical findings were evaluated. Analysis of variance was used to compare preoperative, six-month postoperative and twelve-month postoperative data. The first six mini-pigs grew for six months after instrumentation, and the latter six mini-pigs grew for twelve months after instrumentation[30].

#### *Results.*

The radiographic data collected preoperatively, immediately after the operation and monthly, demonstrated the significant growth of the Cobb angles on the sagittal plane in two groups of animals. For the six month group, the growth of the curve was from  $0^{\circ}\pm 2^{\circ}$  preoperatively to  $13^{\circ}\pm 4^{\circ}$  after six months. For the twelve month group the angles were  $0^{\circ}\pm 2^{\circ}$  preoperatively,  $15^{\circ}\pm 4^{\circ}$  after six months and  $30^{\circ}\pm 13^{\circ}$  after a twelve month period. There was no significant change in angles on the sagittal plane before and after the instrumentation in both groups. Vertebral body wedging, with decreased height on the side of the tether, was observed starting one month postoperatively and progressed over each animal's survival period. Preoperative vertebral body wedging was significantly less than that observed at six or twelve months ( $p \leq 0.001$ ), and wedging observed at twelve months was significantly greater than that observed at six months ( $p \leq 0.001$ ).

#### *Conclusion*

This study confirms the ability of a flexible tether, either steel or polyethylene attached to the vertebral bodies anteriorly, to limit adjacent vertebral growth. This is comparable to how physal-bridging staples alter growth in long bones.

### *Bovine model*

The second study held by this group of researches was called “Spinal growth modulation with an anterolateral flexible tether in an immature bovine model”. An immature bovine model was used to evaluate multilevel anterolateral flexible tethering in a growing spine. In 17 calves, a vertebral staple and two 6.5 mm wide and 45 mm long titanium cancellous vertebral screws were placed with bicortical fixation. Two nontensioned 3/16“ stainless steel cables were placed to connect both sets of screws at all four levels and secured with set screws. For each animal, dorsoventral and lateral radiographs of the thoracic spine were taken immediately after surgery and after harvest. Vertebral body height and width, and disc height measurements were performed. Computed tomography (CT) was performed on 11 spines [30].

### *Results*

After six months of growth, the control group continued to have essentially no coronal or sagittal deformity ( $3.9^{\circ} \pm 3.9^{\circ}$  and  $1.4^{\circ} \pm 3.3^{\circ}$ , respectively). Deformities were created in all spines in the tether group in both the coronal plane and sagittal plane (on average  $37.6^{\circ} \pm 10.6^{\circ}$  and  $18.0^{\circ} \pm 9.9^{\circ}$ , respectively). Over a six month period, vertebral body heights in the control group grew an average of 9.7 mm  $\pm$  2.0 mm per level, resulting in a 34% length increase over the four surgical levels. Final average vertebral body width was 33.5  $\pm$  2.5 mm. Control disc thickness increased 100% over these six months (from an average of 2.1  $\pm$  0.2 mm to 4.0  $\pm$  0.4 mm). Immediate postoperative radiographs showed no differences in initial Cobb measurements between the control and tether groups in either the coronal or sagittal planes. After six months of growth, the control group continued to have essentially no coronal or sagittal deformity ( $3.9^{\circ} \pm 3.9^{\circ}$  and  $1.4^{\circ} \pm 3.3^{\circ}$ , respectively).

Deformities were created in all spines in the tether group in both the coronal plane and sagittal plane (on average  $37.6^{\circ} \pm 10.6^{\circ}$  and  $18.0^{\circ} \pm 9.9^{\circ}$ , respectively). Over six months, vertebral body heights in the control group grew an average of  $9.7 \text{ mm} \pm 2.0 \text{ mm}$  per level, resulting in a 34% length increase over the four surgical levels. Final average vertebral body width was  $33.5 \pm 2.5 \text{ mm}$ . Control disc thickness increased 100% over these six months (from an average of  $2.1 \pm 0.2 \text{ mm}$  to  $4.0 \pm 0.4 \text{ mm}$ ).

### *Conclusion*

Radiographic analysis in this study confirmed the creation of a coronal and sagittal plane spinal deformity over the six month growth period. The double tether construct provided appropriate fixation in the vertebral bodies and consistently created notable vertebral wedging compared with controls.

### **1.3.3 Donita Bylski-Austrow, Eric Wall et al.**

This group of researchers from the department of orthopaedics, Cincinnati Children's Hospital Medical Center, used a porcine model to test the hypothesis that scoliotic curvatures may be repeatedly created using anatomically based vertebral staples and thoracoscopic surgical procedures [32-34]. Custom spine staples were implanted into the midthoracic spines of seven domestic pigs, weighing 240 to 334N (54–75 lbs), which corresponds to approximately three to four months of age. Six staples (per pig) were implanted into the left side of adjacent vertebrae across discs T6–T7 to T11–T12 using a thoracoscopic procedure. Each staple spanned one intervertebral disc and two growth plates just anterior to the rib heads. Each staple was fixed to the vertebral bodies using two bone screws. Following surgery, the animals were maintained for eight weeks. Anteroposterior, lateral, and right oblique (staple true view) radiographs were taken immediately after surgery, at two, four, six, and eight weeks, and again after spine harvest..

### *Results*

In the coronal view, Cobb angles in the remaining five animals at the beginning of the study and at two, four, six and eight weeks were  $0.8^{\circ}$  ( $\pm 1.8$ ),  $5.1^{\circ}$  ( $\pm 2.0$ ),  $7.3^{\circ}$  ( $\pm 1.1$ ),  $9.1^{\circ}$  ( $\pm 2.3$ ), and  $16.4^{\circ}$  ( $\pm 5.4$ ), respectively. Cobb angles at eight weeks in vivo were significantly different than the immediate postoperative values ( $P < 0.01$ ). Radiographs taken after the spine harvest gave better image quality and control. In these, Cobb angles averaged  $22.4^{\circ}$  ( $\pm 2.8$ ) without load and  $21.4^{\circ}$  ( $\pm 4.0$ ) with applied moment; the negligible difference of  $1^{\circ}$  ( $\pm 2$ ) indicated that the curves were not flexible. The angles measured after harvest were markedly different than initial values ( $P < 0.0001$ ). The largest curvatures occurred in the right oblique plane, perpendicular to the staples. Angles at 0, 2, 4, 6 and 8 weeks were  $7^{\circ}$  ( $\pm 2.6$ ),  $11^{\circ}$  ( $\pm 5.6$ ),  $12.6^{\circ}$  ( $\pm 9.4$ ),  $12.5^{\circ}$  ( $\pm 7.0$ ), and  $17.8^{\circ}$  ( $\pm 10.5$ ), respectively. Following the spine harvest, Cobb angles averaged  $26^{\circ}$  ( $\pm 8.7$ ) and curvatures were significantly different than initial values ( $P < 0.01$ ).

### *Conclusion.*

Spinal hemiepiphysiodesis using custom staples with bone screw fixation and minimally invasive surgical procedures repeatedly induced coronal plane spine curvature in a live porcine model. Mean sagittal plane curvature did not increase with postoperative time. If eventually successful clinically, these techniques may slow the progression of, or perhaps even correct, spine deformity without arthrodesis [34].

### **1.3.4 Randal R. Betz MD et al.**

Several studies have been published by this group of researchers describing the use of stapling methods for the treatment of patients with adolescent idiopathic scoliosis [34-37]. This was a retrospective review of patients who had undergone vertebral stapling for treatment of AIS (Figure 1.15), either as a primary treatment or as an alternative to their current treatment of bracing. Inclusion criteria for this review are onset after nine years of age and skeletally immature with a Risser sign  $\leq 2$ . Twenty-one consecutive patients met

the inclusion criteria and have had vertebral body stapling of 27 curves. The preoperative curves ranged from  $18^{\circ}$  to  $52^{\circ}$ . The average age at surgery was 12.0 years (range 10–14 years). This group of 21 patients was analyzed for feasibility and safety. Ten patients with at least a follow-up and preoperative curves  $< 50^{\circ}$  will be analyzed to determine the success of the procedure. The staple is inserted into the pilot holes, the position is confirmed with fluoroscopic image. The pilot holes for a second two prong staple, to be placed posterior to the first staple, can be seen.

### *Results.*

Feasibility was demonstrated in each patient as surgery was successful for the placement of staples at every planned level. Two patients had only one staple placed, instead of two, at the upper thoracic level because of small vertebral body size.



*Figure 1.8. Vertebral body stapling (adapted from [36]).*

No patient required conversion to open thoracotomy for placement of staples. There were no major complications and just three minor complications (14%) in the stapling group. One patient had a segmental spinal vein that was punctured by a staple prong, requiring conversion of the thoracoscopic portal to a mini-incision and ligation of the vein. A second patient developed a chylothorax from a staple prong puncture of the thoracic duct at T12. One patient developed pancreatitis. For the 10 patients evaluated for utility, the average preoperative curve measured  $35 \pm 3.7^{\circ}$  (range  $28^{\circ}$ – $40^{\circ}$ ) and average follow-up curve



measured  $37 \pm 10.2^\circ$  (range  $22^\circ$ – $55^\circ$ ). After 1-year follow-up, the change in the curves ranged from a decrease of  $16^\circ$  to an increase of  $19^\circ$ . Three of the six had significant improvement: Case 1,  $16^\circ$  Case 2,  $8^\circ$ ; and Case 8,  $11^\circ$ . Four of the 10 (40%) showed progression of  $19^\circ$ ,  $10^\circ$ ,  $10^\circ$ , and  $7^\circ$ , respectively. One of the 10 (10%) progressed beyond  $50^\circ$ ; this patient underwent surgery for progression of her thoracic curve.

### **1.3.5 Ian A.F. Stokes et al.**

Based on the author's previous studies of the bone growth modulation, the aim of this study [39] was to document the alteration of growth at two different anatomical growth plate locations, for three differing levels of sustained stress, in three different species, and for animals of differing ages. Growth plates at two anatomical sites (proximal tibia, and caudal vertebra) were subjected to sustained compression or distraction stress in three animal species (rat rabbit, calf), using an external loading apparatus. The tibial growth plate only was used in rabbits, while both growth plates (tail vertebral and proximal tibial) were used in rats and calves. In rats and rabbits, two ages of animals were studied, with older animals having about 75% of the growth rate of younger animals. The sustained stress magnitudes applied to each loaded growth plate had target values of either 0.1 MPa (distraction), 0 MPa (sham), 0.1 MPa (compression) or 0.2 MPa (high compression). The contralateral tibia and adjacent unloaded vertebrae provided internal controls for each animal, while the animals that had the apparatus installed, without spring forces, provided the sham. Thus, data were included in this study from 41 rats, 39 rabbits and 18 calves.

#### *Results*

In most cases the growth plates under tensile stress had increased growth relative to controls (the two younger rats' growth plates were the exception), but this finding was complicated by the 'sham' effect (altered growth associated with application of the loading apparatus, but without loads applied). Generally, the sham-loaded growth plates were observed to have lesser growth rates than their controls. After compensating for the 'sham'

effect by subtracting the mean value from each of the corresponding values for loaded growth plates, growth decreased on average by between 2 and 38 % in the nominally 0.1 MPa compression groups, and decreased by between 19 and 61 percent in the nominally 0.2 MPa compression groups. It was increased by 2 to 36 % for distracted growth plates.

### *Conclusion*

The relationship between actual stress and percentage growth modulation (percent difference between loaded and control growth plates) appeared to be linear, and quantitatively similar. Relationships were found for all three species, for different ages of animals, and at both anatomical locations, although a substantial difference between tibiae and vertebrae was determined. All groups had a significant correlation between growth alteration and stress. As expected, distraction accelerated growth and compression slowed growth. Doubling the compressive stress approximately doubled the proportional reduction in growth rates[39].

## **1.4 General conclusion**

We undertook this study in order to determine the impact of the implantation of SMA (shape memory alloy) staples on the vertebral growth. Using the series of control radiographs as well as the histological analyses of vertebral growth plates we tried to observe both : macroscopic (experimental scoliosis) and microscopic (bone growth rate) responses of the porcine vertebral column to the insertion of SMA. It was the first study of its kind, which combined one side vertebral body stapling with the mentioned earlier methods of control.

## CHARTER 2 Objective and Hypothesis

The goals of this study is to demonstrate that unilateral vertebral body stapling can create an experimental scoliosis curve more then  $5^{\circ}$  and affects vertebral growth causing the decrease of more then 20% of growth rate comparatively to the control group.

In order to confirm the above statements we had to fulfill several objectives:

- 1) Elaborate the optimal surgical procedure, including surgical approach, methods of anaesthesia and post-operative management of animals;
- 2) Choose the method of growth plate labelling, using the recent experiments held in our center and several control labellings;
- 3) Make a histological analyses of vertebral body growth plates for every group of animals in order to estimate an compare the growth rates between them.

## CHARTER 3 Materials and Methods

### 3.1 Introduction

In this chapter we will review the methods, animal models and materials used in this study.

### 3.2 Animal model

The animal model of the Landrace domestic pig (Figure 3.1) was selected for the present study. The reasons for such a selection are based on several anatomical and physiological similarities between a human adolescent and a domestic pig, including the size of the thoracic vertebrae. The concentrated growth of female pigs from three months of age to sexual maturity at six months of age is comparable to human bone growth during adolescence, but in a much shorter period of time.



*Figure 3.1: Experimental animal.*

The twelve female Landrace domestic pigs, three months of age, arrived one week prior to surgery in order to pass a necessary quarantine. The animals were treated according to

protocols approved by the institutional committee of good practice in research at Saint-Justine Hospital based on the norms established by the Canadian Council on Animal Care (CCAC).

The animals were divided into three groups:

1. The first group, composed of six pigs, were instrumented using 10mm U-shape Ni-Ti SMA staples and instruments for their application designed by Medtronic Sofamor-Danek (Memphis, USA).
2. The second group of three animals were used as the sham group in order to study the influence of a surgical procedure on bone growth without staple placement.
3. The third group of three animals were used as the control group.

The Ni-Ti (Nitinol) SMA memory alloy staples (Figure 3.2) used in this study are U-shaped implants with four prongs joined with a laminar bridge portion including an aperture at its center.



*Figure 3.2: Memory alloy staple*

Nitinol's properties are derived from a reversible, solid state phase transformation known as a martensitic transformation [40]. At high temperatures, Nitinol assumes an interpenetrating simple cubic crystal structure referred to as austenite (also known as the parent phase). At low temperatures, Nitinol spontaneously transforms to a more complicated "monoclinic" crystal structure known as martensite. The temperature whereby

austenite transforms to martensite is generally referred to as the transformation temperature. More specifically, martensite begins to form at the so-called Ms temperature, and is considered complete at the Mf temperature. Crucial to Nitinol's properties are two important aspects of this phase transformation. First, the transformation is "reversible" meaning that heating above the transformation temperature will revert the crystal structure to the simpler austenite phase. Upon heating, however, there is a slight upward shift in the temperatures, now beginning at the As temperature, and finishing at the Af temperature. The second key point is that the transformation in both directions is instantaneous. Martensite's crystal structure (known as a monoclinic, or B19' structure) has the unique ability to undergo limited deformation, about a 6-8% strain, without breaking atomic bonds. When martensite is reverted to austenite by heating, the original austenitic structure is returned, regardless of whether the martensite phase was deformed. Thus, the name "shape memory" refers to the fact that the shape of the high temperature austenite phase is "remembered," even though the alloy is severely deformed at a lower temperature. A great deal of force can be produced by preventing the reversion of deformed martensite to austenite, in many cases, more than 100,000 psi. In an ordinary alloy, the constituents are randomly positioned on the crystal lattice, however since Nitinol is an intermetallic compound, the atoms (in this case, nickel and titanium) have very specific locations in the lattice.

### **3.3 Surgical protocol**

The pigs fasted for a period of twelve hours preoperatively. For transport, the animals were placed in a restraining cage and the following sedative medications were injected fifteen minutes prior to surgery: atropine 0.04mg/kg, azaperone 4.0mg/kg, ketamine 25mg/kg IM via a 21G catheter.

Once asleep, the animal was covered with a blanket and transported to the department of experimental surgery (9<sup>th</sup> floor, Block 9). The animal was then placed on the

surgical table equipped with a heating mat in the prone position. Following the anaesthesia, delivered by mask using Isoflurane 2.5% / L O<sub>2</sub>, an intravenous catheter (22G) was inserted in the ear vein and held in place with tape. During the surgery 0.9% NaCl was administered intravenously at a rate of 10ml/kg/hour. Injection of propofol (10 mg/ml, dose: 1.66mg/kg) was made via IV catheter. Following the loss of reflex (relaxation of the jaw), the pig was intubated (xylocaine spray to the vocal cords and introduction of the endotracheal tube sized between 5.5 and 6.5) using a laryngoscope and connected to the respirator for anaesthesia maintenance through the flow of 10ml/kg anaesthetic gas (mixture of Isoflurane 1.5% / litre of oxygen). Throughout the surgery both the heart rate and oxygen saturation were monitored.

In order to properly identify one animal from the next, each pig was assigned a number by place of a tag through a hole in the ear. The animal was placed in the left lateral position and attached to the surgical table with pull strings. The conductive cauterisation plate was placed on the right hip and the surgical site was shaved and cleaned with chlorhexidine solution and Betadine. The level of anaesthesia was continuously verified through stimulation of the nasal septum or the anal sphincter. A sterile field was placed over the pig's chest revealing only the surgical site.

An incision was made in the seventh intercostal space on the right chest wall. Until the pleural cavity, all tissue layers were passed using a thorough haemostasis. The use of the costal retractor provided the space required for passage of the graft instruments. Previously cooled to 0°C, sterile Ni-Ti staples were expanded and implanted to enclose two adjacent growth plates spanning an intervertebral disc space at five different thoracic levels from T6 to T11.

Animals from the sham group underwent identical surgical procedure exclusive of staple insertion. Rather, four holes were made in the cortical bone tissue at the same level as the instrumented group. The surgery was finished by thorough closure of the wound by means of absorbable and non-absorbable suture filaments.

The wound was covered with Opsite spray and a Fentanyl patch (7.5mg) was applied on the ear as an analgesic. The animals also received the antibiotic Excenel

(3mg/kg) administered intravenously in the neck 24 hours prior to surgery and two days following the surgery. Postoperatively, the pigs were held in communal cages of four.

### 3.4 Radiographic control

The radiographs were generated biweekly, for a period of eight weeks postoperatively, and on the day of sacrifice (five in total) under general anaesthesia using the same sedative mixture administered during surgery (atropine 0.04mg/kg, 4.0mg/kg azaperone, 100mg/ml ketamine 25mg/kg IM via 21G catheter). Concomitantly, the pigs were weighted in order to calculate the necessary medication dosage.

Two radiographic views were taken every time and included posterior-anterior and lateral (Figure 3.3.).

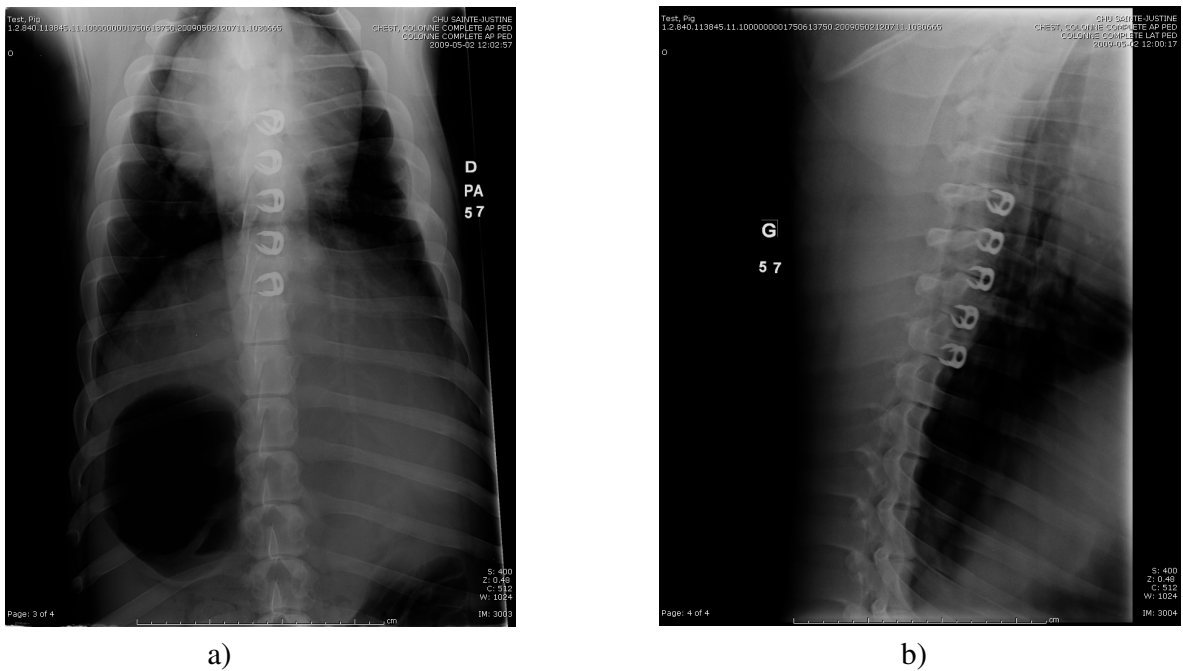


Figure 3.3 (a, b): Posterior-anterior (a) and lateral (b) radiographs of porcine spine.



These goal of the postoperative images are to provide a constant control for staple position, measurement of Cobb's angle and wedging of vertebrae in order to compare data between all experimental groups. The measurements were performed via the programme Synapse 3.1.1.

### **3.5 Growth plate labelling.**

Following two previous test studies of bone growth labelling, the decision was made to use Calcein Sigma (Fluorescein-bis (methyliminodiacetic acid)) as a growth labelling agent. The approved standard protocol for bone labelling was used. The concentration of calcein used in this study was 20 mg/kg, in order to ensure prominent fluorescent lines under the microscope. A mixture of calcein and sodium bicarbonate ( $\text{NaHCO}_3$ , 10 mg/kg) was dissolved in 500 ml of 0.9% NaCl. Previously sedated animals, having had the same sedation for the surgery and radiographs, were injected slowly into the ear vein with a labelling mixture using a simple Manifold. In total two injections of calcein six days apart were made, one on the seventh day and one 24 hours prior to sacrifice.

At the end of the study, once the animals reached six months of age, the pigs were sedated using Ketamine and then euthanized using Euthanyl 240 mg/kg intravenously. Following the euthanasia, a spinal segment containing vertebrae T6 to T11 was dissected from each animal. Excessive connective and bone tissues were removed and the blocks of vertebrae were immersed in 10% solution of formaldehyde.

#### **3.5.1 Plasticisation of vertebrae and cutting**

In order to have thin slices of vertebrae for the microscopy, the harvested vertebrae should be impregnated in MMA (methyl methacrylate) solution. For this purpose, all of the harvested samples have passed through the following steps of tissue preparation for plasticisation presented in the Table 3.1 below. After plasticisation, which can take from one to three weeks, the blocks of paired vertebrae were cut using an Isomet 1000 precision

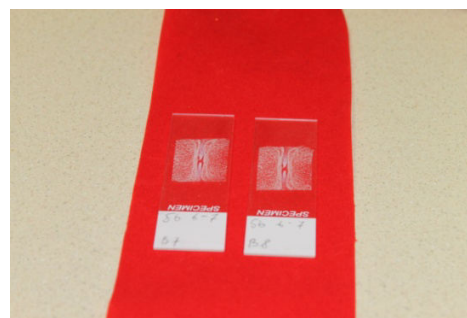
saw to form brick shaped blocks of two vertebrae containing two neighbourhood growth plates and an intervertebral disc between them. Two sequences (sequence A and B) of 6 micrometer thin sections were cut on each vertebra-disc-vertebra bloc at the level of ventral prongs (sequence A) and between ventral and dorsal prongs (sequence B) using Leica SM2500 Microtome (Figure 3.4 and 3.5). Each sequence consists of 10 sections made 25 micrometres apart.

*Table 3.1. Plasticisation of vertebrae*

Solution	Time of exposure
Initial buffered Formol	24 (change the solution if it turns red)
Buffered Formol	1 to 3 day(s)
Buffered Formol	3 to 5 days
Buffered Formol	3 to 5 days
Alcohol 80%	one day and one night (3 changes)
Alcohol 95%	one day and one night(2 changes)
Alcohol 100%	3-5 days (4 changes)
Xylene	7-9 hours (4 changes)
MMA0%	3-5 days (2 changes)
MMA1%	5-7 days (2 changes)
MMA3.8%	9-11 days (3 changes)
MMA3.8%	Final solution



a)



b)

Figure 3.4 ( a, b). Vertebra-disc-vertebra bloc (a) and sections (b).

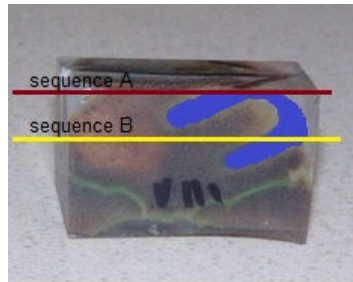


Figure 3.5. Sequences A and B.

### 3.5.2 Growth rate measurement

The cut sections were evaluated under the fluorescent optic microscope Leica DMR using a polarised filter for calcein and a UV lamp. In order to understand how compressive forces created by shape memory alloy staples are distributed on the subjacent tissues, every growth plate was virtually divided into four zones, zone 4 being closest to the staple and zone 1 the furthest (Figure 3.6). The average daily growth rate was calculated by measuring the distance between the two fluorescent lines on the growth plate (Figure 3.7), in micrometres, and dividing the number by six, the number of days between calcein injections. These measurements were executed using custom software. The average growth rates were calculated for every zone over each vertebra in all three groups of animals.

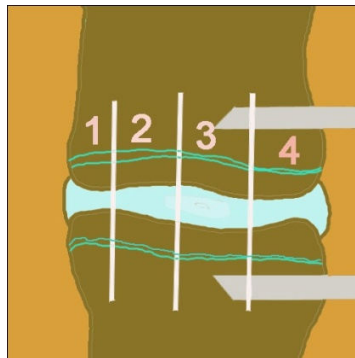
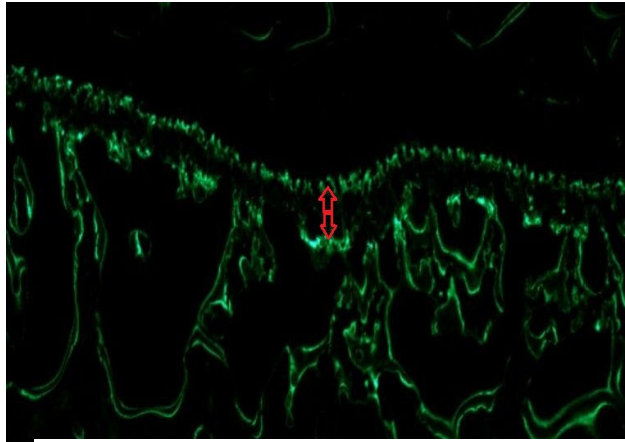


Figure 3.6: Four zones of growth plates



*Figure 3.7. Two fluorescent lines of calcein*

### **3.6 Statistical analyses**

In order to confirm or disapprove our scientific hypothesis we made a post-hoc analyses of both: Cobb angles and growth rates which were compared between groups using values recorded pre-operatively and immediately prior to euthanasia. Because of the number of experimental animals we used non-parametric Wilcoxon tests to interpret these data using SPSS software. Group sample sizes were determined using a significance of  $\alpha=0.05$  and a power of  $p=0.80$ . Measures (Cobb angles and growth rates) were repeated by two different observers [41].

## CHAPTER 4 Scientific article

The contribution of the first author of the article is about 70 % (tissue processing, growth rate and Cobb angle measurements, preparation for the surgery), Isabelle Villemure (scientific background of the study, study design), Mark Driscoll (assistance in the surgery, statistics), Stefan Parent (scientific background of the study, study design, performance of the surgery, study management). The article is submitted **on the xx of xxxx 2012** for the publication in *Spine*, the journal of Lippincott Williams & Wilkins.

### 4.1 Characterization of in vivo vertebral growth modulation by shape memory alloy staples on a porcine model for the correction of the scoliosis



**Characterization of in vivo vertebral growth modulation by shape memory alloy staples on a porcine model for the correction of the scoliosis**

Yaroslav Wakula, MD<sup>1,2</sup>, Isabelle Villemure, Eng., Ph.D.<sup>2,3</sup>,  
Mark Driscoll, Eng., Ph.D.<sup>2,3</sup>, Stefan Parent MD, Ph.D.<sup>1,2</sup>

*1- Université de Montréal  
P.O. Box 6128, Station "Centre-Ville"  
Montréal, QC H3C 3J7*

*2- Sainte-Justine University Hospital Center  
3175 Côte-Ste-Catherine Rd.  
Montréal, Québec, H3T 1C5, Canada*

*3- Dept. of Mechanical Engineering, École Polytechnique of Montreal  
P.O. Box 6079, Station "Centre-Ville"  
Montréal, Québec, H3C 3A7, Canada*

**Authors' e-mail addresses:**

Yaroslav Wakula

Mark Driscoll

Stefan Parent

Isabelle Villemure

**Corresponding author:**

Stefan Parent, MD, PhD

Hôpital Ste-Justine

3175 Côte Ste-Catherine, room 7904

Montréal, Québec

H3T 1C5

### 4.1.1 Structured Abstract

*Study Design:* Twelve Landrace domestic pigs were instrumented using memory shape alloy (SMA) staples to evaluate their ability to impose growth modulation on thoracic vertebrae.

*Objective:* Evaluate the growth modulation potential of SMA staples on thoracic vertebral growth plates in control, sham, and instrumented groups by means of measured radiological changes.

*Summary of Background Data:* Over the past few decades, numerous published studies have proposed different growth modulation approaches with the objective of correcting idiopathic scoliosis without fusion. However, measures of growth rate changes caused by SMA staples have yet to be evaluated in a large animal model.

*Methods:* A group of six three month old female domestic pigs was instrumented using 10mm U-shape Ni-Ti memory alloy staples at the thoracic level from T6 to T11. Three animals underwent surgery without vertebral body stapling (sham group), while two animals served as a control. Postoperatively, posterior-anterior (PA) and lateral (LAT) radiographs of the thoracic spine were taken biweekly. After a period of three months, a bone labelling agent (calcein) was injected intravenously at eight and two days prior to sacrifice. In order to measure the growth rate, two thin slide sequences at the level of the ventral prongs (sequence A) and between ventral and dorsal prongs (sequence B) of all involved growth plates were evaluated under fluorescent microscope.

*Results:* A scoliosis curve ( $5.8 \pm 3.2$ ) developed in all instrumented animals. For sequence A, mean growth rates reached  $12.73 \pm 3.9$ ,  $19.03 \pm 1.8$  and  $18.97 \pm 1.96 \mu\text{m/day}$  for the instrumented, sham and control groups respectively. Correspondingly, the rates of sequence B were  $12.47 \pm 2.9$ ,  $20.01 \pm 1.84$  and  $19.26 \pm 2.2 \mu\text{m/day}$ .

*Conclusion:* Vertebral stapling induced spinal curvatures and decreases vertebral growth rate in the instrumented animals. Optimal positioning of the staple is essential for bone growth modulation and development of experimental scoliosis. Bone growth is mostly affected immediately underneath the staple.

**Key Words:** shape memory alloy staples, growth modulation, fusionless treatment, scoliosis

### 4.1.2 Introduction

Conventional treatments of idiopathic scoliosis comprise predominantly bracing and open correction of the deformity. The former is used to treat scoliotic curves with a Cobb angle up to 40°, while the latter is reserved for severe cases and entails a permanent implantation of spinal instrumentation with vertebral fusion. Since their introduction, both methods have proven effective. However, despite evident positive characteristics, these methods can pose a significant number of undesirable effects to patient health. Bracing is a long term treatment implemented over a period of one to two years and requires the permanent wearing of an orthosis, which proves both physically and psychologically challenging for the patient<sup>1</sup>. The shortcomings corresponding to open reduction of scoliotic curves are obviously more severe and include important surgical intervention, significant blood loss, high cost of the procedure, and permanent vertebral fusion. These inadvertent and concurrent side effects set it amongst the surgical treatments with the most significant long-term impact in orthopedic surgery.

For these reasons, fusionless techniques offer a prospective alternative to traditional treatments of scoliosis. Fusionless techniques present significantly less surgical risk and complication than conventional methods through the maintenance of disc mobility. To date, there exist different technical approaches proposed in order to correct the deformity while maintaining the natural flexibility of the spine. Betz R. et al. used SMA staples to treat scoliosis in young patients<sup>2</sup> and promoted their technique as an alternative to bracing<sup>1</sup>. Conversely, Wall E. et al.<sup>3</sup> used their implants on a porcine model as an alternative to open reduction<sup>4</sup>. Other methods of creating experimental scoliosis included the use of flexible or rigid tethers<sup>5</sup>. However, these studies did not evaluate the impact of implants on the growth rate of vertebrae in large animals. Such data could be essential in understanding the distribution of load on the growth plates of instrumented vertebrae. Moreover, it may provide confirmation that the Hueter-Volkman law, which correlates bone growth rate to local loading, plays an important role in the development of scoliosis.

Therefore, the goal of this research is to create a scoliosis curve using SMA staples and to measure the growth rate on the growth plates of thoracic vertebrae of pigs. Similar



studies on bovine and rat tails<sup>6,7</sup> demonstrated a slowing of bone growth up to 30% compared to control animals. It is expected that this research will yield similar results.

### **4.1.3 Materials and methods**

The animal model of the Landrace domestic pig was selected for the present study. The reasons for such a selection are based on several anatomical and physiological similarities between a human adolescent and a domestic pig, including the size of the thoracic vertebrae. The concentrated growth of female pigs from three months of age to sexual maturity at six months of age is comparable to human bone growth during adolescence, but in a much shorter period of time.

The twelve female Landrace domestic pigs, three months of age, arrived one week prior to surgery in order to pass a necessary quarantine. The animals were treated according to protocols approved by the institutional committee of good practice in research at Saint-Justine Hospital based on the norms established by the Canadian Council on Animal Care (CCAC).

The animals were divided into three groups:

1. The first group, composed of six pigs, were instrumented using 10mm U-shape Ni-Ti SMA staples and instruments for their application designed by Medtronic Sofamor-Danek (Memphis, USA).
2. The second group of (n=3) were used as the sham group in order to study the influence of a surgical procedure on bone growth without staple placement.
3. The third group (n=2) animals were used as the control group.

The Ni-Ti (Nitinol) SMA memory alloy staples used in this study are U-shaped implants with four prongs joined with a laminar bridge portion including an aperture at its center.

#### 4.1.3.1 Surgical Protocol

The pigs fasted for a period of twelve hours preoperatively. After the sedation with ketamine, atropine and azaperone each animal was covered with a blanket and transported to the department of experimental surgery. There, the surgery was performed under the general anaesthesia delivered by mask using Isoflurane 2.5% / L O<sub>2</sub> and intravenous propofol. In order to properly identify one animal from the next, each pig was assigned a number by place of a tag through a hole in the ear.

An incision was made in the seventh intercostal space on the right chest wall. The pleura was incised and the thoracic cavity was entered. The use of the costal retractor provided the space required for passage of the instruments. Previously cooled to 0°C, sterile Ni-Ti staples were expanded and implanted to enclose two adjacent growth plates spanning an intervertebral disc space at five different thoracic levels from T6 to T11 (Figure 4.1).

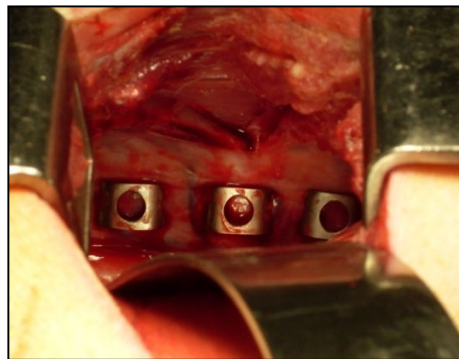


Figure 4.1 : Insertion of the staples

The surgery was finished by thorough closure of the wound by means of absorbable and non-absorbable suture filaments. The wound was covered with Opsite spray and a Fentanyl patch (7.5mg) was applied on the ear as an analgesic. The animals also received the antibiotic Excenel (3mg/kg) administered intramuscularly in the neck 24 hours prior to surgery and two days following the surgery. Postoperatively, the pigs were held in

communal cages of four. Animals from the sham group underwent identical surgical procedure exclusive of staple insertion. Rather, four holes were made in the cortical bone tissue at the same level as the instrumented group.

#### **4.1.3.2 Radiographic control**

The radiographs were acquired biweekly over eight weeks postoperatively and on the day of sacrifice (five in total) under general anaesthesia using the same sedative mixture utilized during the surgery (atropine, azaperone and ketamine). Concomitantly, the pigs were weighted in order to calculate the necessary medication dosage. Two radiographic views were taken every time and included posterior-anterior and lateral. These images are to provide a constant control for staple position, measurement of Cobb's angle and wedging of vertebrae in order to compare these data between all experimental groups. All measurements were performed via the programme Synapse 3.1.1.

#### **4.1.3.3 Bone growth labelling and tissue preparation**

Calcein Sigma (Fluorescein-bis (methyliminodiacetic acid)) was used as a bone growth labelling agent. Two intravenous injections of calcein at the dose of 20 mg/kg were subsequently administered eight and two days prior to sacrifice. At the end of the study, once the animals were six months of age, the pigs were sedated using Ketamine and then euthanized using Euthanyl 240 mg/kg intravenously. Following the euthanasia, a spinal segment containing vertebrae T6 to T11 was dissected from each animal. Excessive connective and bone tissues were removed and the blocks of vertebrae were immersed in 10% solution of formaldehyde. Each block was divided into five segments containing two adjacent growth plates and the adjoining intervertebral disc. In order to have a thin slice of vertebrae for the microscope, all segments were impregnated with MMA (methyl methacrylate) solution. Two sequences (A and B) of six micrometer thin sections were cut on each vertebra-disc-vertebra bloc at the level of ventral prongs (sequence A) and between

ventral and dorsal prongs (sequence B) (Figure 4.2) using Leica SM2500 Microtome. Each sequence consisted of ten sections taken twenty-five micrometres apart.

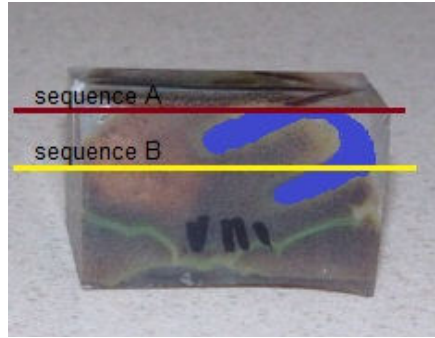


Figure 4.2. Two sequences of sections.

#### 4.1.3.4 Growth rate measurement

The cut sections were evaluated under the fluorescent optic microscope. Every growth plate was virtually divided into four zones, zone four being closest to the staple and zone one the furthest (Figure 4.3).

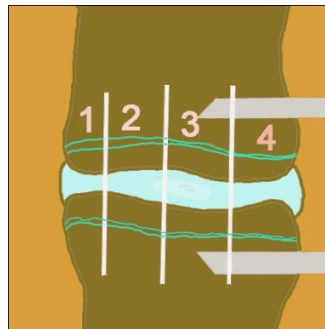


Figure 4.3: Four zones of growth plate

The growth rate was calculated by measuring the distance between the two created fluorescent lines in the growth plate (Figure 4.4) in micrometres and dividing the number by six, the number of days between calcein injections. These measurements, in micrometers per day, were executed using custom Matlab 7.0 software. The average growth rates were calculated for every zone over each vertebra in all three groups of animals.

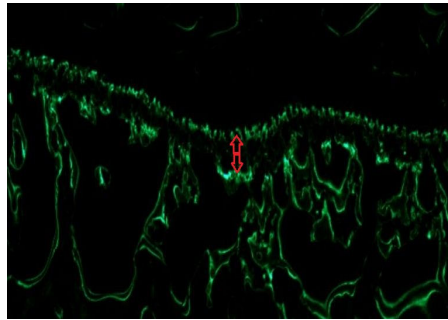


Figure 4.4: Growth plate under the microscope

#### 4.1.3.5 Statistical analyses

Group sample sizes were determined using a significance of  $\alpha=0.05$  and a power of  $p=0.80$ . Post-hoc analyses were compared between groups using values recorded pre-operatively and immediately prior to euthanasia (Cobb angles). Non-parametric Wilcoxon tests were utilized to interpret this data. Measures (Cobb angles and growth rates) were repeated by two different observers.

#### 4.1.4 Results

The estimated blood loss during the operation was 20-40 ml. Minor infection at the site of operation occurred in two instrumented animals. One of these animals was euthanized as a result of severe infection during the post-operative period. Consequently, data received from this animal were excluded from the analysis. A decision was made to operate on one animal from the control group in order to maintain six instrumented porcine. Thus, the study persisted with 11 experimental animals, including six instrumented, three sham and two control pigs.

#### 4.1.4.1 Radiographs

Radiographs taken immediately following the operation did not reveal, in all three groups of animals, any considerable angular deviation of the spine on the posterior-anterior images. Table 4.1 demonstrates no development of significant scoliotic curves within the control group when comparing initial and final radiographs ( $p=1.0$ ).

Table 4.1. Cobb angle in all groups

Group	Animal	Cobb angle before treatment	Cobb angle after treatment
Instrumented	1	1°	6°
	2	0°	4°
	3	0°	7°
	4	0°	9°
	5	2°	3°
	6	0°	6°
Sham	1	1°	0°
	2	0°	0°
	3	0°	0°
Control	1	0°	0°
	2	0°	0°

The same statement holds true for the sham group ( $p=0.51$ ). Final radiographs of the instrumented group demonstrate the development of significant scoliotic curves compared to initial images ( $p<0.05$ ) with an average Cobb angle of  $5.8^{\circ} \pm 3.2^{\circ}$ . The comparison of final Cobb measures between all three groups revealed a significant difference between the instrumented group and both the control and sham groups ( $p=0.04$  and  $0.02$  respectively) and the absence of an insignificant difference between the sham and control groups ( $p \geq 0.5$ ). Further analyses of radiographs revealed that a considerable number of staples were displaced with respect to the ideal position. Spinal columns in which the SMA staples were most accurately positioned demonstrate the greatest Cobb angles. As an example we can take animal 4, which developed a scoliotic curve of  $9^{\circ}$  (most significant in loaded group).

Evaluation under the microscope revealed an accurate positioning of the staples as compared with the other animals.

#### **4.1.4.2 Bone growth measurement**

The average growth rate in the control group measured both from sequence A and B was  $19.4 \pm 2.2$   $\mu\text{m}/\text{day}$ . No significant variation of the growth rate, measured across the four growth plate zones within the control group, was observed. Results obtained from the sham group were similar to those of the control group. An average growth rate of  $19.5 \pm 1.8$   $\mu\text{m}/\text{day}$  was documented without notable distribution differences of the growth rate in all four growth plate zones. The comparison between these two groups showed no statistically significant differences between growth rate measurements ( $p=0.73$  and  $0.62$  for the sequence A and B respectively). As for the instrumented group, the average growth rate was measured at  $12.6 \pm 3.9$   $\mu\text{m}/\text{day}$ . To better understand the pattern in which the insertion of the staples modifies the growth rate, the average growth rates in zone three and four from the instrumented group (just beneath the prong of staples) were compared with the respective values from the control and sham groups. The statistical analyses for these data showed the instrumented group's growth rate of  $10.88 \pm 5.23$  to be significantly less than the sham's at  $19.1 \pm 2.1$   $\mu\text{m}/\text{day}$  ( $p < 0.01$ ) and the control's at  $19.14 \pm 1.99$   $\mu\text{m}/\text{day}$  ( $p < 0.01$ ) for the sequence A. Sequence B yielded similar results. The mean instrumented group's growth rate of  $11.04 \pm 3.9$   $\mu\text{m}/\text{day}$  was significantly less than the sham's at  $20.02 \pm 2.04$   $\mu\text{m}/\text{day}$  ( $p < 0.01$ ) and the control's at  $19.74 \pm 2.11$   $\mu\text{m}/\text{day}$  ( $p < 0.01$ ). However, there is considerable variation in the growth rate between different growth plates in each experimental animal.

#### **4.1.5 Discussion**

The comparative analyses of radiographs and growth plate labelling between control and sham groups revealed no significant differences, indicating that the surgical procedure itself does not affect the vertebral growth. On the other hand, the presence of SMA staples

led to the creation of significant scoliotic curves in four of six instrumented animals and considerable slowing of bone growth (up to 33%) in comparison to control and sham groups. Similar studies performed on a rat model<sup>1,2</sup> had approximately the same difference between growth rates in control and instrumented groups. However, certain technical difficulties were encountered during this experimentation. Due to the relatively small incision and the absence of radioscopic control during the surgical procedure not all staples were placed accurately around the two adjacent growth plates and intervertebral disc. This explains why Cobb angles did not reach significant degrees in all experimental animals as well as the discrepancy in growth rate measurements in the instrumented group. The key factor that influenced the modification of the growth rate was the position of the staple. The accurate positioning of the staple also led to an unequal distribution of the load on a plate, resulting in the highest growth rate measured in zone one and the lowest growth rate measured in zone four. The discrepancy in growth rates between different zones is presented on a graph below (Figure 4.5).

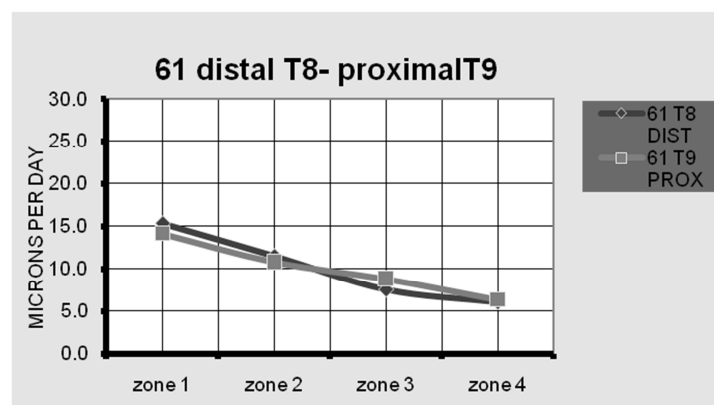


Figure 4.5. Distribution of the growth rate in 4 zones.

Nonetheless, the spines with precisely inserted staples demonstrated the development of significant curves and slowing of bone growth. The development of relatively small scoliotic curves in comparison to those in other similar studies<sup>3,4</sup> can be explained by the constructive differences of implants used and the smaller number of instrumented vertebrae. Porcine spines, due to their physiological characteristics, tend to be a good experimental model. The size and the form of porcine vertebrae are similar to those



in humans and rapid growth during the first six months of life closely mimic patterns experienced during the adolescent growth spurt. However, being a quadruped animal, the pigs experience less axial stress<sup>5</sup> on their spinal column and have a more rigid rib cage which can influence the final outcome of an experiment.

In conclusion, the present study demonstrates the *in vivo* potential of SMA staples to modulate vertebral growth by creating scoliotic curves on radiographs and by slowing the growth rate on instrumented growth plates. Accurate positioning of the SMA staple is essential for optimal bone growth modulation and the corresponding development of experimental scoliosis. Growth modulation predominantly takes place directly underneath the staple prongs (zone 4). For further studies, it is recommended to explore a more effective method of accurate staple insertion and to increase the number of instrumented vertebrae.

#### 4.1.6 References:

1. Guille James T., D'Andre Linda P. a, Betz Randal R., Fusionless Treatment of Scoliosis. *Orthop Clin N Am* 38 (2007) 541–545
2. Betz Randal R., MD, John Kim, MD,† Linda P. D'Andrea, MD, M. J. Mulcahey, MS, Rohinton K. Balsara, MD, and David H. Clements, MD An Innovative Technique of Vertebral Body Stapling for the Treatment of Patients With Adolescent Idiopathic Scoliosis: A Feasibility, Safety, and Utility Study. *Spine* Volume 28, Number 20S, pp S255–S265.
3. Wall E, Bylski-Austrow D, Kolata R, et al. Endoscopic mechanical spinal hemiepiphysiodesis modifies spine growth. *Spine* 2005; 30(10): 1148-53
4. Bylski-Austrow D, Wall E., David L. Glos, Edgar T. Ballard, Andrea Montgomery and Alvin H. Crawford Spinal Hemiepiphysiodesis Decreases the Size of Vertebral Growth Plate Hypertrophic Zone and Cells. *J Bone Joint Surg Am.* 2009;91:584-593. doi:10.2106/JBJS.G.01256

5. Newton P, Upasani V, Farnsworth C, et al. Spinal growth modulation with the use of a tether in an immature porcine model. *J Bone Joint Surg Am* 2008; 90: 2695-706
6. Stokes IA, Aronsson DD, Dimock AN, Cortright V, Beck S: Endochondral growth in growth plates of three species at two anatomical locations modulated by mechanical compression and tension. *J Orthop Res.* 2006;24(6):1327-34
7. Cancel, M., Grimard, G., Thuillard-Crisinel, D., Moldovan F. & Villemure, I. (2009) Effects of in vivo static compressive loading on aggrecan and type II and X collagens in the rat growth plate extracellular matrix. *Bone*, 44(2), 306-15. Epub 2008 Sep 24.
8. Bylski-Austrow D, Glos D, Sauser F, et al. Bilateral intra-annular spinal compressive stresses in vivo. *Stud Health Technol Inform* 2006; 123: 398-40

## CHAPTER 5 Results

### 5.1 General information

One of the original pigs from the loaded group was euthanized and excluded from the study because of severe postoperative infection, which could not be treated with antibiotics. The decision to sacrifice the animal was made to relieve its suffering. The second animal from the same group demonstrated significant displacement of the staples that made a calculation of the growth rate impossible, however radiographic data from the animal were included in the study. In order to maintain six animals in the loaded group, a pig from the control group was operated on. Thus, the final number of animals was 11, including six loaded, three sham and two control.

### 5.2 Radiographic control

Radiographs taken immediately following the operation didn't reveal, in all three groups of animals, any considerable angle deviation of the spine on the posterior-anterior and lateral images (Figure 5.1).

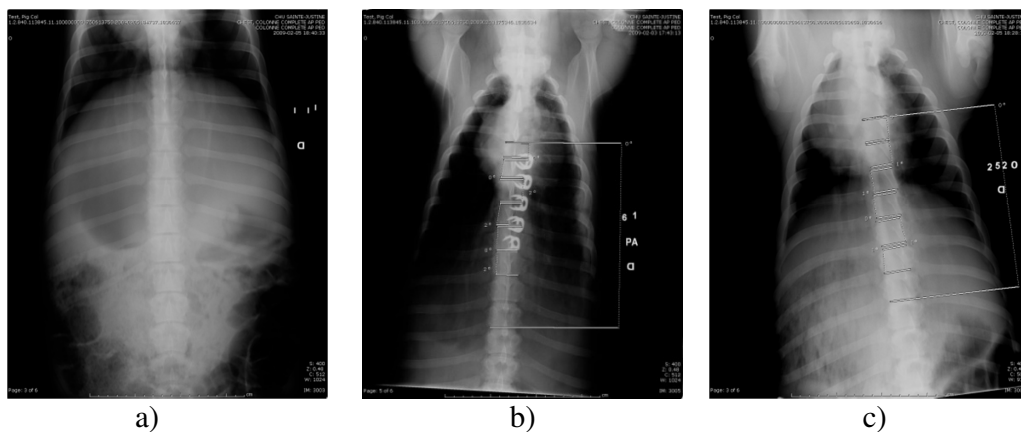


*Figure 5.1(a,b,c):* The initial PA radiographs of thoracic spine of animals from a) control, b) loaded and c) sham groups.

The analysis of initial and final radiographs for all groups of animals revealed no development of significant scoliosis curves in the control group ( $p=1$ ), the same results were obtained for the sham group ( $p=0.51$ ). The comparison of final Cobb angles for the loaded group indicated a development of significant scoliosis curves in the final radiographs ( $p<0.05$ ), compared to initial images with an average Cobb angle of  $5.8^{\circ} \pm 3.2^{\circ}$ .

The comparison of final results between all three groups revealed a significant difference between the loaded group and both the control and sham groups ( $p=0.04$  and  $0.02$  respectively), and an insignificant difference between the sham and control groups ( $p \geq 0.5$ ). The results of radiological control are presented in their entirety in Table 5.1. Visual analysis of radiographs revealed that a considerable number of staples were displaced with respect to the ideal position. Spinal columns where staples were most accurately positioned demonstrated greater Cobb angles.

*Table 5.1. Cobb angles in three groups of animals.*

Group	Animal	Cobb angle beginning of study	Cobb angle end of study
Loaded	1	1°	6°
	2	0°	4°
	3	0°	7°
	4	0°	6°
	5	2°	3°
	6	0°	9°
Sham	1	1°	0°
	2	0°	0°
	3	0°	0°
Control	1	0°	0°
	2	0°	0°

### 5.3 Bone growth measurement

As seen in the article, we obtained the decrease of the bone growth in the loaded group of animals, for which the average growth rate was measured at  $12.6 \pm 3.9 \mu\text{m/day}$ . Which gives us 35.7% decrease of the growth rate when compared with the control group and 35.4% decrease in comparison with the sham group. The comparison of the growth rate data between control and sham groups showed no significant differences between growth rate measurements ( $p=0.73$  and  $0.62$  for the sequence A and B respectively). Table 5.2 and Figure 5.2 are demonstrating the comparison of the growth rate between three groups of

*Table 5.2. Average growth rate in three groups of animals.*

Average growth rate in all zones			
Experimental group	Control	Sham	Loaded
Growth rate (micrometres/day)	19.4	19.5	12.6

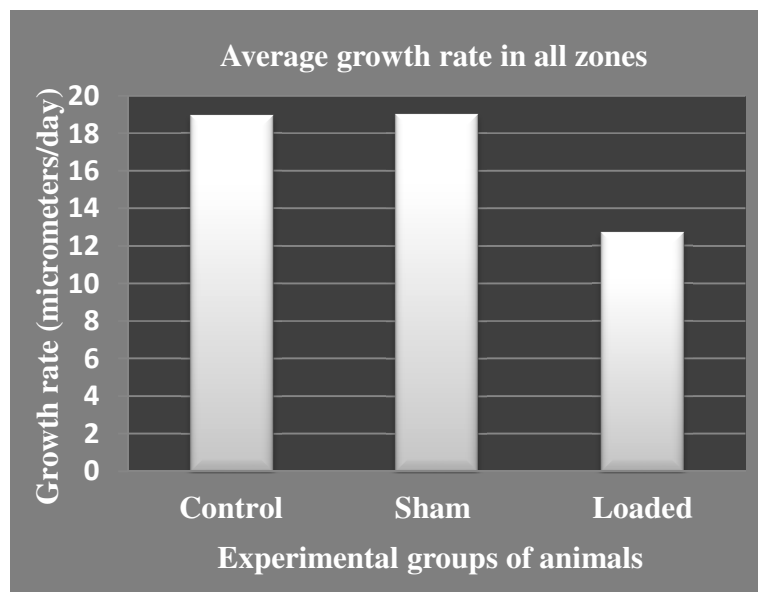


*Figure 5.2: Diagrams representing an average growth rate in three groups of animals.*

In the result section of the same article we showed the growth rate values obtained in different zones of the growth plate (more precisely in zones 3 and 4). Even more significant decrease of growth rate in loaded group was observed in these zones when compared with respective zones of control and sham groups. The average growth rate in zones 3 and 4 was less up to 43.5% then in sham and control groups. The results were very similar for both: sequence A and sequence B. Figure 5.3 and Table 5.3 are representing the average growth rate in zones 3 and 4 for all three groups of animals

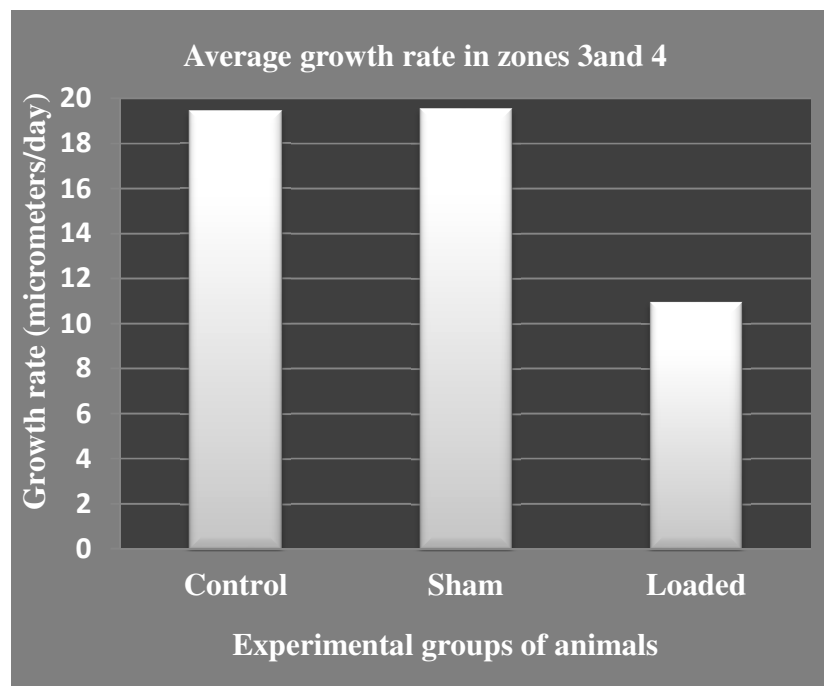


*Figure 5.3. Diagrams representing an average growth rate in three groups of animals (zones 3and4).*

Table 5.3. Average growth rate in three groups of animals(zones 3 and 4) .

Average growth rate in zones 3 and 4			
Experimental group	Control	Sham	Loaded
Growth rate micrometres/day	19.44	19.56	10.96

However, there is considerable variation in the growth rate between different growth plates in each experimental animal. The key factor that influenced the modification of the growth rate was the position of the staple. The accurate positioning of the staple also led to an unequal distribution of load on a plate, resulting in the highest growth rate measured in zone 1 and the lowest growth rate measured in zone 4 (closest to the staple). The discrepancy in growth rates between different zones on a loaded growth plate is presented on graphs below (Figure 5.4 and 5.5).

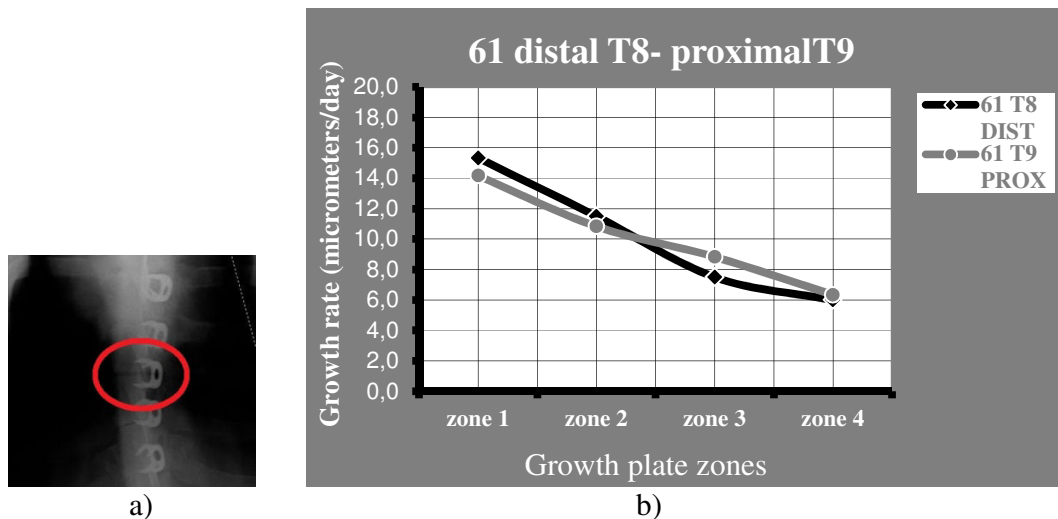


Figure 5.4: Accurate positioning (a) of the staple has resulted in notable decrease (b) of growth rate in two neighbor growth plates.

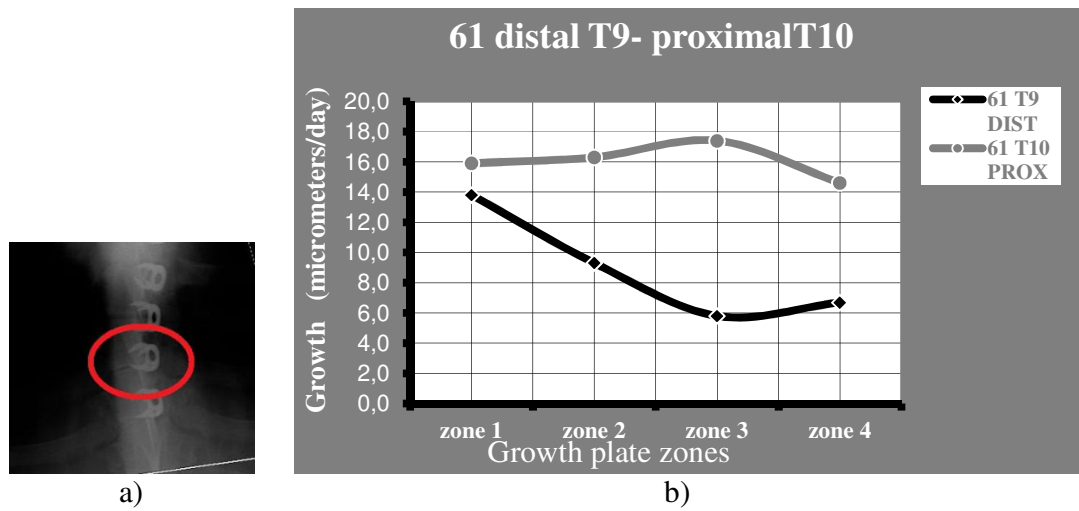


Figure 5.5: The staple is displaced (a). Only the distal T9 growth plate was compressed (b).

Thus our results showed that the position around two growth plates is very important in order to obtain a maximum decrease of the growth rate. In the next chapter we will discuss the results of this study.



## CHAPTER 6 Discussion

The aim of the present study was to estimate the ability of memory alloy staples to modify the growth of thoracic vertebrae by creating local compression of two neighbouring growth plates around which every staple was inserted. In order to characterise those modifications two methods were selected, namely a series of radiographs and growth plate labelling. In addition, the study also attempted to understand what supplementary factors (i.e. surgical techniques, position of the staple or local tissue reaction) could influence the final results. The analysis of radiographs and growth plate labeling has led to the following statements:

- The insertion of memory alloy staples affects the growth rate. The lowest growth rate was obtained in zone 4, which represents the closest part of the growth plate just beneath the staple;
- The calculation of the bone growth rate also revealed a decrease of bone growth in the loaded group, which is significantly different from the data obtained from both the sham and control animals;
- The insertion of memory alloy staples created a significant scoliosis curve in four of six animals from the loaded group when compared with the sham and control groups;
- The comparison of both sets of data (radiographs and bone labelling) showed no notable difference between the sham and control groups, meaning that the surgical procedure did not influence the growth of vertebrae;
- The variability of data obtained from the loaded group can be explained by the fact that, objective reasons (small incision, structural characteristics of animal), not all staples were positioned precisely around two adjacent growth plates;

In general, the two hypothesis were tested and proven. A considerable slowing of average bone growth was obtained in the loaded group (up to 35.7%) compared to the control and sham groups, and even more (up to 43.5%) in zones 3 and 4. These results are compatible with similar studies by Cancel [42] and Stokes [39] on the rat model, which had

a decrease from 15 to 29% and from 2 to 38% respectively. Together with the works of mentioned authors this is another useful contribution for better understanding of the bone growth modulation.. The analysis of post operative radiographs revealed that only four of six loaded animals developed a significant scoliosis curve superior to 5°. Though the creation of scoliosis was a desirable part of this study and reflects the ability of vertebral stapling to modify the longitudinal growth of vertebrae, it is not considered the main goal of this research. The development of relatively small scoliosis curves, in comparison to those obtained in other similar studies held by Wall [34] (average Cobb angle of  $22.4^{\circ} \pm 2.8^{\circ}$ ) could be explained by differences in an implants design, more rigid fixation of the implants using screws, and an increased number of instrumented levels involved in their studies. Due to a relatively small incision and the absences of radiosopic control during the surgical procedure, not all staples were placed accurately around two neighboring growth plates and intervertebral disc.

The importance of accurate staple insertion is demonstrated through the data obtained from animal six in the loaded group. On the column of this animal, the staples are positioned more precisely than in the other loaded spines, leading to the development of the largest scoliosis curve ( $9^{\circ}$ ) of the entire experiment (Figure5.1).



*Figure 6.1.* Final PA radiograph of thoracic spine of animal 6. The presence of  $9^{\circ}$  scoliosis curve.

The Porcine spine, due to its physiological characteristics, is considered to be a good experimental model. The size and the form of porcine vertebrae are similar to those in humans and rapid growth during the first six months of life closely mimic patterns experienced during the adolescent growth spurt. However, being a quadruped animal, the pig experiences less axial stress on its spinal column and has a more rigid rib cage which can influence the final outcome of the experiment.

## CHAPTER 7 Conclusion

The selection of experimental animal, materials, methods of bone growth labeling and operative technique used in this study has allowed the *in vivo* demonstration of shape memory alloy staple potential to modulate vertebral growth. This was supported by the staples ability to create scoliotic curves, confirmed via radiograph analyses, and by slowing the vertebral growth rate of instrumented growth plates. Several test animals were used to establish optimal techniques for bone labeling in large animals, such as pigs, as well as the necessary time delay between two injections of labeling agents (calcein). According to common scientific practice, the study incorporated three groups of experimental animals: control, sham and loaded. A sham group was included to prove the surgical procedure, without insertion of the staple, does not affect the vertebral bone growth. Results of both radiological control and bone growth labeling obtained in all three groups were compared using non-parametric Wilcoxon tests. The data from the loaded group were statistically different from those of control and sham groups. The main hypothesis was verified and the lowest growth rate was observed in the loaded group. Nevertheless, difficulties during the study were encountered which included the inaccurate position of a considerable number of staples in the loaded group. No radioscopy control during the surgical procedure was available and only a relatively small incision in the thorax provided the surgical viewing field. Consequently, these limitations perhaps led to inaccurate staple insertion, the most distant vertebra from the incision being the most difficult. Utilizing a small incision operative approach was dictated by the risk of post operative septic complications. Despite these shortcomings, results obtained in the loaded group demonstrated a statistically significant decrease in the average growth rate and development of scoliotic curves when compared with control and sham groups.

The staples showed their ability to create enough compressive force between the prongs to locally (zones 3 and 4) reduce the growth of vertebra by up to 33%; however, it is believed that the high rigidity of the porcine thoracic spine hindered the staple's performance and allowed only for the creation of scoliotic curves up to 9°.

The obtained results and difficulties encountered during this study have allowed for the elaboration of several recommendations for further scientific explorations:

- Improve operative techniques in order to more precisely control the insertion of implants by improving visualization. This may be achieved by making a wider surgical approach or using two incisions in the thorax.
- Increase the number of experimental animals in order to have more statistically robust data.
- Increase the number of instrumented vertebrae in order to produce a bigger scoliotic curve in loaded animals.
- Search for an experimental animal with a less rigid thorax or loosen the rigidity by costotomy or costectomy.
- The use of special techniques to create an artificial scoliosis by applying an asymmetric tether, as performed in the study by Braun [29] followed by an insertion of staples in order to understand how the staples will affect the bone growth in conditions which are maximally approached to those seen in scoliotic patients.

The need for improved techniques for the treatment of adolescent idiopathic scoliosis remains a priority due to certain objective limitations of conventional treatments. The use of memory alloy staples seems to be a prospective approach in the treatment of AIS. This study has demonstrated the staple's promising ability to modulate the growth of vertebrae in pigs. However, further investigations are needed in order to elaborate a precise technique of their use in clinical practice.

## References

1. Vasiliadis, E.S., T.B. Grivas, and A. Kaspiris, *Historical overview of spinal deformities in ancient Greece*. *Scoliosis*, 2009. **4**: p. 6.
2. Nachlas, I.W. and J.N. Borden, *The cure of experimental scoliosis by directed growth control*. *J Bone Joint Surg Am*, 1951. **33**(A:1): p. 24-34.
3. Stokes, I.A., *Hueter-Volkman effect*. *Spine*, 2000. **14**: p. 349-357.
4. Stokes, I.A., *Mechanical effects on skeletal growth*. *J Musculoskelet Neuronal Interact*, 2002. **2**(3): p. 277-80.
8. Moore, D.P., A.F. Dalley, and A.M. Agur, *Clinically Oriented Anatomy* 2006: Lippincot, Williams & Wilkins.
6. Available from: <http://www.chiro.org/forms/romchiro.htm>
5. Ballock, R.T. and R.J. O'Keefe, *The biology of the growth plate*. *J Bone Joint Surg Am*, 2003. **85-A**(4): p. 715-26.
6. Villemure, I. and I.A. Stokes, *Growth plate mechanics and mechanobiology. A survey of present understanding*. *J Biomech*, 2009. **42**(12): p. 1793-803.
7. Growth Plate Dynamics. Date of consultation: 30.11.2011 from <http://www.the-scientist.com/article/display/58130/>
9. Soucacos, P.N., et al., *School-screening for scoliosis. A prospective epidemiological study in northwestern and central Greece*. *J Bone Joint Surg Am*, 1997. **79**(10): p. 1498-503.

10. Benoit, P., *Idiopathic Scoliosis. What a resident should know*. 2003, Montreal: Sainte-Justine Hospital.
11. Wynne-Davies, R., *Familial (idiopathic) scoliosis. A family survey*. J Bone Joint Surg Br, 1968. **50**(1): p. 24-30.
12. Machida, M., *Cause of idiopathic scoliosis*. Spine (Phila Pa 1976), 1999. **24**(24): p. 2576-83.
13. Department of Orthopaedic Surgery - University Stellenbosch, South Africa (30.11.2011) Risser's Sign from [www0.sun.ac.za/ortho/webct-ortho/age/risser.html](http://www0.sun.ac.za/ortho/webct-ortho/age/risser.html)
14. Delorme, S., H. Labelle, and C.E. Aubin, *Is Cobb angle progression a good indicator in adolescent idiopathic scoliosis?* Spine (Phila Pa 1976), 2002. **27**(6): p. E145-51.
15. Greiner, K.A., *Adolescent idiopathic scoliosis: radiologic decision-making*. Am Fam Physician, 2002. **65**(9): p. 1817-22.
16. Harms, J. *Spine Surgery Information Portal*. (21.10.2011) Available from: [www.harms-spinesurgery.com](http://www.harms-spinesurgery.com).
17. Carr, W.A., et al., *Treatment of idiopathic scoliosis in the Milwaukee brace*. J Bone Joint Surg Am, 1980. **62**(4): p. 599-612.
18. Goldberg, C.J., et al., *Adolescent idiopathic scoliosis: the effect of brace treatment on the incidence of surgery*. Spine (Phila Pa 1976), 2001. **26**(1): p. 42-7.
19. Scoliosis support group of Queensland. Milwaukee and Boston braces. (12.10.2011). From: <http://www.scoliosissupport.org.au/treatment.htm>.
20. Wever, D.J., et al., *Curve progression and spinal growth in brace treated idiopathic scoliosis*. Clin Orthop Relat Res, 2000(377): p. 169-79.
21. Bridwell, K.H., *Surgical treatment of idiopathic adolescent scoliosis*. Spine (Phila Pa 1976), 1999. **24**(24): p. 2607-16.
22. Dubousset, J., J.A. Herring, and H. Shufflebarger, *The crankshaft phenomenon*. J Pediatr Orthop, 1989. **9**(5): p. 541-50.
23. Mullaji, A.B., et al., *Vertebral growth after posterior spinal fusion for idiopathic scoliosis in skeletally immature adolescents. The effect of growth on spinal deformity*. J Bone Joint Surg Br, 1994. **76**(6): p. 870-6.
24. Pediatric orthopedics. Luque rod system. (23.08.2011). From <http://www.pediatric-orthopedics.com/Treatments/Skeletal/Spine/Scoliosis/Example/example.html>

25. Smith, A.D., W.H. Von Lackum, and R. Wylie, *An operation for stapling vertebral bodies in congenital scoliosis*. J Bone Joint Surg Am, 1954. **36**(A:2): p. 342-8.
26. Braun, J.T., E. Akyuz, and J.W. Ogilvie, *The use of animal models in fusionless scoliosis investigations*. Spine (Phila Pa 1976), 2005. **30**(17 Suppl): p. S35-45.
27. Braun, J.T., et al., *The efficacy and integrity of shape memory alloy staples and bone anchors with ligament tethers in the fusionless treatment of experimental scoliosis*. J Bone Joint Surg Am, 2005. **87**(9): p. 2038-51.
28. Braun, J.T., et al., *Mechanical modulation of vertebral growth in the fusionless treatment of progressive scoliosis in an experimental model*. Spine (Phila Pa 1976), 2006. **31**(12): p. 1314-20.
29. Braun, J.T., et al., *Fusionless scoliosis correction using a shape memory alloy staple in the anterior thoracic spine of the immature goat*. Spine (Phila Pa 1976), 2004. **29**(18): p. 1980-9.
30. Newton, P.O., et al., *Spinal growth modulation with an anterolateral flexible tether in an immature bovine model: disc health and motion preservation*. Spine (Phila Pa 1976), 2008. **33**(7): p. 724-33.
31. Newton, P.O., et al., *Spinal growth modulation with use of a tether in an immature porcine model*. J Bone Joint Surg Am, 2008. **90**(12): p. 2695-706.
32. Bylski-Austrow, D.I., et al., *In vivo compressive stresses in the intervertebral disc, in North American Congress on Biomechanics 2008*: Ann Harbor, MI.
33. Bylski-Austrow, D.I., et al., *Spinal hemiepiphysiodesis decreases the size of vertebral growth plate hypertrophic zone and cells*. J Bone Joint Surg Am, 2009. **91**(3): p. 584-93.
34. Wall, E.J., et al., *Endoscopic mechanical spinal hemiepiphysiodesis modifies spine growth*. Spine (Phila Pa 1976), 2005. **30**(10): p. 1148-53.
35. Betz, R.R., et al., *Vertebral body stapling procedure for the treatment of scoliosis in the growing child*. Clin Orthop Relat Res, 2005(434): p. 55-60.
36. Betz, R.R., et al., *An innovative technique of vertebral body stapling for the treatment of patients with adolescent idiopathic scoliosis: a feasibility, safety, and utility study*. Spine (Phila Pa 1976), 2003. **28**(20): p. S255-65.
37. Betz, R.R. and H. Shufflebarger, *Anterior versus posterior instrumentation for the correction of thoracic idiopathic scoliosis*. Spine (Phila Pa 1976), 2001. **26**(9): p. 1095-100.



38. Guille, J.T., L.P. D'Andrea, and R.R. Betz, *Fusionless treatment of scoliosis*. Orthop Clin North Am, 2007. **38**(4): p. 541-5, vii.
39. Stokes, I.A., et al., *Endochondral growth in growth plates of three species at two anatomical locations modulated by mechanical compression and tension*. J Orthop Res, 2006. **24**(6): p. 1327-34.
40. K. Otsuka, C.M.W., ed. *Shape Memory Materials*. ed. C.U. Press 1998-05-28 298.
41. A., R.B., ed. *Fundamentals of biostatistics*. 7th ed. 2011, Brooks/Cole.
42. Cancel, M., et al., *Effects of in vivo static compressive loading on aggrecan and type II and X collagens in the rat growth plate extracellular matrix*. Bone, 2009. **44**(2): p. 306-15.
43. Motion range of the spine. (11.06.2011) Available from: <http://www.chiro.org/forms>
44. Cervical Spine Anatomy (02.09.2011). .Adapted from <http://www.activemotionphysio.ca/article.php?aid=308>
45. Lumbar spine.(04.05.2011). From <http://www.back.com/anatomy-lumbar.html>
46. Health encyclopedia. Sacrum (04.05.2011). From <http://www.oocities.org>
47. Netter, F.H., *Atlas of Human Anatomy*. 4th ed 2006: Saunders Elsevier..
48. Anatomy of the IV disc (04.05.2011). From <http://www.yourmma.tv/trainingm>

## Annexe 1

### The descriptive anatomy of spine.

The vertebral column functions as a strong pillar for the support of the trunk and the cranium, provides articular surfaces for the attachment of the ribs, and affords protection for the spinal cord and the roots of the spinal nerves. It transmits the weight of the trunk to the inferior extremities. Although forming a continuous support-bearing column, it is flexible enough to permit bending of the trunk in various directions. The vertebral canal, which follows the different curves of the column, accommodates and protects the spinal cord; it is formed by the superimposition of the vertebrae in each of which there is a vertebral foramen. Despite its flexibility, the vertebral column is sufficiently firm and strong to serve as a base of origin for many ligaments and muscles and as a lever for the spinal muscles, which function to maintain the upright position of the trunk [8].

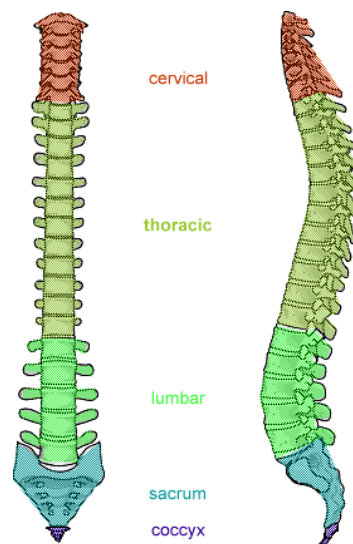


Figure 0 : Schematic image of the spine (adapted from [8]).

The human vertebral column in an adult consists of 33-35 vertebrae arranged in five regions: cervical, thoracic, lumbar, sacral and coccygeal (Fig.A.1).

## Cervical spine

The cervical region consists of seven relatively mobile vertebrae (Figure A.2). Their smaller size reflects the fact that they bear less weight than the larger inferior vertebrae. Although the cervical IV discs are thinner than those of inferior regions, they are relatively thick compared to the size of the vertebral bodies they connect. The relative thickness of the discs, the nearly horizontal orientation of the articular facets, and the small amount of surrounding body mass give the cervical region the greatest range and variety of movement of all the vertebral regions (Table A.1).

*Table A.1. The range of motion in cervical spine (males) (adapted from [43]).*

Motion	Degree
Flexion	50°
Extension	60°
Left Lat Flex	45°
Right Lat Flex	45°
Left Rotation	80°
Right Rotation	80°



Figure A.2 Cervical vertebrae (adapted from [44]).

## Thoracic spine

Thoracic vertebrae (Figure A.3) lie in the upper back. The primary characteristic of these vertebrae are their costal facets for the articulation with ribs. These costal facets and other characteristics are presented below. The middle four thoracic vertebrae (T5-T8) are representative of all the typical features. The articular processes of thoracic vertebrae extend vertically with paired, nearly coronally oriented articular facets that form an arc centered in the IV disc. This arc permits rotation and some lateral flexion of the vertebral column in this region, in fact, the greatest degree of rotation is permitted here. Attachment of the rib cage combined with the vertical orientation of articular facets and overlapping spinous processes limits flexion and extension, as well as lateral flexion. The T1-T4 vertebrae share features of cervical vertebrae, while the T9-T12 vertebrae share features of lumbar vertebrae including tubercles similar to their accessory and mammillary processes [8].

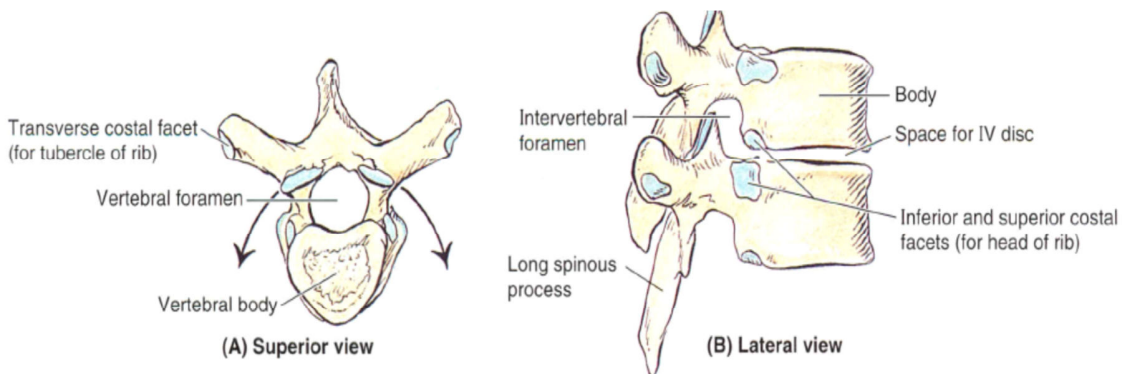


Figure A.3: Thoracic vertebrae (adapted from [8]).

## Lumbar spine.

Lumbar vertebrae are located in the lower back between the thorax and sacrum (Figure A.4). Because the weight they support increases toward the inferior end of the vertebral column, lumbar vertebrae have massive bodies, accounting for much of the thickness of the lower trunk in the median plane. Their articular processes extend vertically, with articular facets sagittally oriented initially (beginning abruptly with the T12-L1 joints) but becoming more coronally oriented as the column descends. The L5-S1 facets are distinctly coronal in orientation [8].



Figure A.4 : Lumbar vertebrae (adapted from [45]).

## Sacrum

The large, triangular, wedged-shaped sacrum is usually composed of five fused sacral vertebrae in adults (Figure A.5). It is located between the hip bones and forms the roof and posterosuperior wall of the posterior pelvic cavity.

## Coccyx

The coccyx (Figure A.5), its name derived through comparison to a cuckoo's beak, is usually formed of four small segments of bone, the most rudimentary parts of the vertebral column. In each of the first three segments may be traced a rudimentary body, articular and transverse processes; the last piece (sometimes the third) is a mere nodule of bone, without distinct processes. All the segments are devoid of pedicles, laminae, and spinous process, and, consequently, of intervertebral foramina and spinal canal

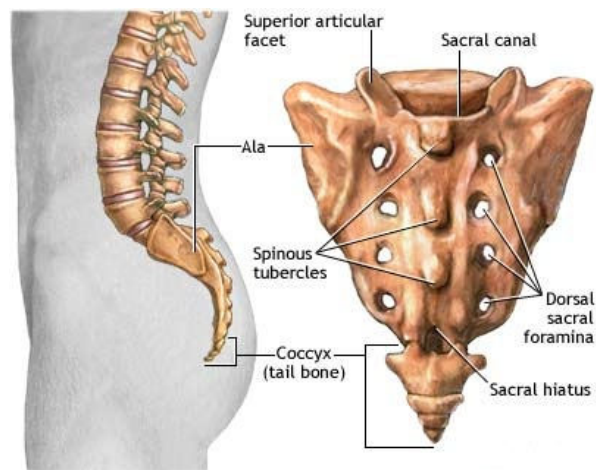


Figure A.5 : Sacrum and Coccyx (adaped from [46]).

Significant motion occurs only between the 25 superior vertebrae. Of the nine inferior vertebrae, the five sacral vertebrae are fused in adults to form the sacrum and, after approximately age of 30, the four coccygeal vertebrae fuse to form the coccyx. The lumbosacral angle occurs at the junction of, and is formed by, the long axes of the lumbar region of the vertebral column and the sacrum. The vertebrae gradually become larger as the vertebral column descends to the sacrum, and then become progressively smaller toward the apex of the coccyx. This change in size is related to the fact that successive vertebrae bear an increasing amount of the body's weight as the column descends. The vertebrae reach maximum size immediately superior to the sacrum, which transfers the weight to the pelvic girdle and the sacroiliac joints. The vertebral column is flexible

because it consists of many relatively small bones, called vertebrae (singular = vertebra), that are separated by resilient IV discs. The 25 cervical, thoracic, lumbar, and first sacral vertebrae also articulate at synovial zygapophysial joints, which facilitate and control the vertebral column's flexibility. Although the movement between two adjacent vertebrae is small, in aggregate the vertebrae and IV discs uniting them form a flexible yet rigid column that protects the spinal cord they surround [47].

### Structure and function of intervertebral discs

The disc consists of a nucleus pulposus and an anulus fibrosus (Figure A.6). The superficial layers of the anulus have been cut and spread apart to show the direction of the fibers. It is important to note that the combined thickness of the rings of the anulus is diminished posteriorly, in other words the anulus is thinner. The fibrogelatinous nucleus pulposus occupies the center of the disc and acts as a cushion and shock-absorbing mechanism. The pulpy nucleus flattens and the anulus bulges when weight is applied, as occurs during standing and more so during lifting.

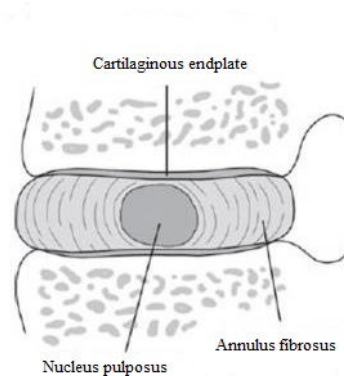


*Figure A.6: Structure of intervertebral discs (adapted from [48]).*

During flexion and extension movements, the nucleus pulposus serves as a fulcrum. The anulus is simultaneously placed under compression on one side and tension on the other [47].

## Ligaments of the spine

The ligaments of the spine maintain a crucial role in the stability and function of the vertebral column. The ligaments are not only responsible for keeping the components of the entire structure together, but are also fundamental in permitting movement of the spine. They serve as strings that prevent excessive movement of the column and, by storing elastic energy, help the muscles to regain an upward position of the spine making them more efficient. The main ligaments (Figure A.7) of Spinal Column (SC) are outlined below:

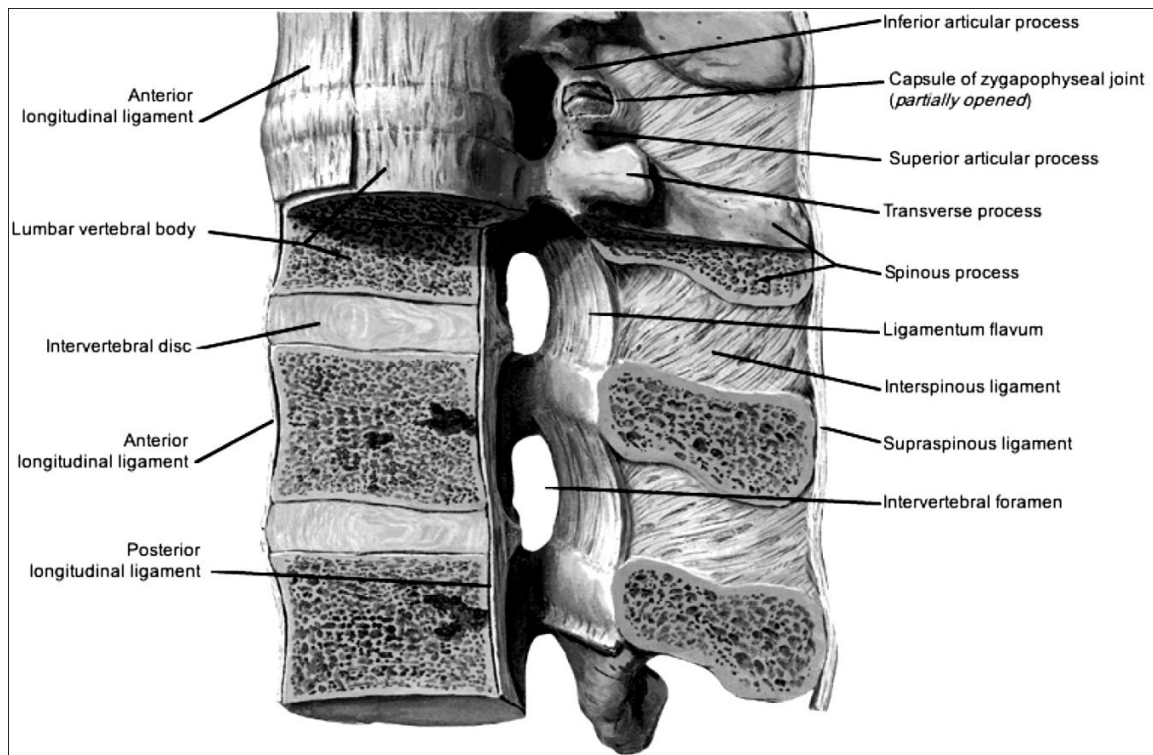


Figure A.7: Ligaments of the spine (adapted from [47]).

- The anterior longitudinal ligament runs from the base of the skull along the front of each vertebral body and disc and down the anterior sacrum. It resists backward bending and limits the forward curve of the neck and lumbar regions.



- The posterior longitudinal ligament runs along the back aspect of the vertebral bodies and discs and down into the canal that lies within the sacrum. It tightens with forward bending.
- The facet joint capsule, a balloon like structure that wraps around each facet joint, has sensory receptors that guide the movement between adjacent vertebrae.
- The ligamentum flavum connects the back of the vertebral arches and forms the back wall of the spinal canal. It is known as the yellow ligament because of the colour imparted by the preponderance of elastic fibers. Off to the sides, it fuses with the facet joint capsules. In the midline, it turns posteriorly to become the interspinous ligament. Lengthened by flexion (forward bending) of the spine, its elastic fibers supply a strong returning force.
- The interspinous ligament runs between the spinous processes. Its anterior fibers are rich in elastin and blend with the ligamentum flavum, while the posterior fibers blend with the supraspinous ligament.
- The intertransverse ligaments bind the ends of the transverse processes and resist side bending to the opposite side.
- The supraspinous ligament connects the tips of the spinous processes and goes on to join with the thoracolumbar fascia [47].